



Contents lists available at ScienceDirect

Science of the Total Environment

journal homepage: [www.elsevier.com/locate/scitotenv](http://www.elsevier.com/locate/scitotenv)

## Evaluating MONICA's capability to simulate water, carbon and nitrogen fluxes in a wet grassland at contrasting water tables

Valeh Khaledi<sup>a,b,\*</sup>, Roland Baatz<sup>a</sup>, Danica Antonijević<sup>a</sup>, Mathias Hoffmann<sup>a</sup>,  
Ottfried Dietrich<sup>a</sup>, Gunnar Lischeid<sup>a,c</sup>, Mariel F. Davies<sup>a</sup>, Christoph Merz<sup>a</sup>, Claas Nendel<sup>a,b,d</sup>

<sup>a</sup> Leibniz Centre for Agricultural Landscape Research (ZALF), Eberswalder Str. 84, 15374 Müncheberg, Germany

<sup>b</sup> Institute of Biochemistry and Biology, University of Potsdam, Am Mühlenberg 3, 14476 Potsdam, Germany

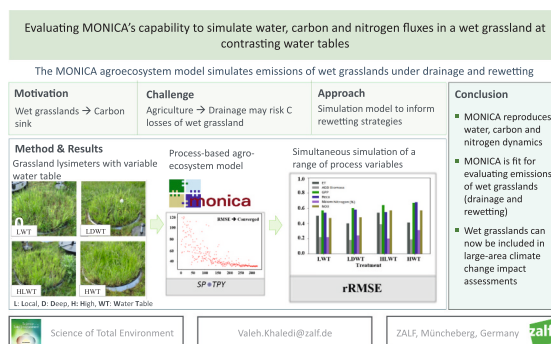
<sup>c</sup> Institute of Environmental Science and Geography, University of Potsdam, Karl-Liebknecht-Str. 24-25, 14476 Potsdam, Germany

<sup>d</sup> Global Change Research Institute, Czech Academy of Sciences, Bělidla 986/4a, 603 00 Brno, Czech Republic

### HIGHLIGHTS

- Wet grasslands are hotspots for biodiversity, nutrient turn-over and gas emissions.
- Groundwater level dynamics determine water, carbon and nitrogen cycles.
- We used the MONICA agroecosystem model to simulate grassland lysimeter processes.
- MONICA was tested against CO<sub>2</sub> exchange, evapotranspiration and nitrogen emissions.
- MONICA captures well the groundwater influence on the biogeochemical processes.

### GRAPHICAL ABSTRACT



### ARTICLE INFO

Editor: Jurgen Mahlknecht

#### Keywords:

Wet grasslands  
Carbon sink  
Nitrogen loss  
MONICA  
SPOTPY algorithm

### ABSTRACT

Wet grasslands, which are vital for water and nutrient regulation, are characterised by distinct water, carbon (C) and nitrogen (N) dynamics, and their interactions. Due to their shallow groundwater table, wet grasslands promote a strong interconnection between diverse vegetation and soil water. Researchers have investigated how wet grasslands respond to environmental changes, using various simulation models to understand how these sites contribute to water, C and N dynamics. However, a comprehensive, simultaneous study of all three of these dynamics is still lacking. This study makes use of a grassland lysimeter study with differently managed groundwater levels and employs the process-based Model for Nitrogen and Carbon dynamics in Agroecosystems (MONICA) to simulate these dynamics. By using SPOTPY (Statistical Parameter Optimization Tool) to optimise the relevant parameters, we find that MONICA performs well in simulating vegetation growth (aboveground biomass), and elements of the water (evapotranspiration), C (gross primary productivity, ecosystem respiration) and N (N in aboveground biomass, nitrate in soil solution, Nitrous oxide emissions) balance, with Willmott's Refined Index of Agreement always larger than 0.35. This level of accuracy demonstrates that MONICA is ready to be applied for scenario simulations of groundwater management and climate change to evaluate their impact

\* Corresponding author at: Leibniz Centre for Agricultural Landscape Research (ZALF), Eberswalder Str. 84, 15374 Müncheberg, Germany.

E-mail address: [valeh.khaledi@zalf.de](mailto:valeh.khaledi@zalf.de) (V. Khaledi).

<https://doi.org/10.1016/j.scitotenv.2024.174995>

Received 15 February 2024; Received in revised form 16 July 2024; Accepted 21 July 2024

Available online 23 July 2024

0048-9697/© 2024 The Authors. Published by Elsevier B.V. This is an open access article under the CC BY license (<http://creativecommons.org/licenses/by/4.0/>).

on greenhouse gas emissions and long-term carbon storage, as well as water and nitrogen losses in wet grasslands.

## 1. Introduction

Grasslands provide up to 40 % of renewable ecosystem services globally (Zedler and Kercher, 2005), including as a significant source of food for livestock, and habitat space for a wide range of animal and vegetation species (Bengtsson et al., 2019). Grasslands sites encompass a wide spectrum of hydrological conditions, ranging from permanently inundated wetlands (e.g. reed swamps) to dry grasslands with insufficient water availability. These hydrological conditions define the vegetation (Joyce et al., 2016). Wet grasslands are defined as permanent grasslands that experience groundwater influence or significant precipitation input throughout the year that leads to predominantly moist (i.e. up to or beyond field capacity) topsoil and occasional flooding (Joyce et al., 2016). Wet grasslands have a continuously changing soil moisture content, ranging from dry to completely saturated, resulting in heterogeneity in anoxic and oxic conditions at aggregate scale in the soil. For these reasons, they are hotspots for biogeochemical transformations, allowing for a wide range of biochemical reactions (Ramsar Convention Secretariat, 2010). Furthermore, the species composition in wet grasslands responds very quickly to fluctuations in the groundwater table (Khaledi et al., 2024), with additional implications for the soil's chemistry. In Europe, wet grassland accounts for a most vulnerable fraction of the organic carbon (C) stored in soils under agricultural use, which has been subjected to massive degradation as a consequence of draining in recent years. In the search for potential C sequestration options to meet the climate protection goals of the Paris Agreement under the United Nations Framework Convention on Climate Change (UNFCCC, 2015), wet grasslands have recently come into focus (UNFCCC, 2022).

In wet grassland ecosystems, the dynamics of the diverse vegetation plays an essential role in regulating the cycles of water, C and nitrogen (N) (Wassen et al., 2013). The composition and productivity of plant biomass influences the water budget through evapotranspiration (ET), and the water supply, in turn, impacts productivity. Soil moisture is an important regulator of the C and N turnover in soil, and N availability to vegetation (Lohse et al., 2009; Oleson et al., 2008; Rodriguez-Iturbe et al., 2001). Litterfall from vegetation returns nutrients to the soil, making the grassland ecosystem a comparably rapid nutrient cycle (Cong et al., 2014), if not interrupted as a result of biomass offtake, e.g. haymaking on meadows. Understanding how wet grassland ecosystems respond to changes in environmental conditions is key to comprehending (i) their contribution to water losses, greenhouse gas (GHG) emissions, and nitrate (NO<sub>3</sub><sup>-</sup>) leaching, and (ii) how these responses can be controlled through appropriate groundwater management (Mitsch and Gosselink, 2015; Wang et al., 2020). Currently, the groundwater table (and thus the water supply) of a major proportion of wet grasslands under agricultural production is managed using weirs and dams (Die-trich et al., 2012).

The balance and cycle of the water, C and N components at wet grassland sites has already been covered in a wide range of studies. Most of them have addressed the importance of the soil's biogeochemical processes in storing and releasing C and N (Raich and Nadelhoffer, 1989; Schimel, 2013; Schmidt et al., 2011; Trumbore and Czimczik, 2008). In addition, the influence of factors such as agricultural and water management (Edwards et al., 2023; Li et al., 2017) and climate (Gibson and Newman, 2019), as well as the presence of specific plant species (Mayel et al., 2021) has been extensively explored. Most of these studies, however, have looked at the aforementioned aspects in isolation. What is still missing at this point is a comprehensive study that thoroughly examines the interconnectivity of water, C and N fluxes in wet grassland ecosystems.

Process-based simulation models simulate the dynamics of agro-ecosystems and their underlying biogeochemical processes. They have been acknowledged to be potent tools for investigating C and N cycles (Abramoff et al., 2018; Chang et al., 2015; Fatichi et al., 2019; Wang et al., 2013). Process-based models are built from differential equations that describe the water, C and N fluxes in an agroecosystem, and subsequently their interaction through plant and soil. The majority of models have employed the pool concept (Hénin and Dupuis, 1945; Jenkinson and Rayner, 1977), as it is implemented in the CENTURY (Parton et al., 1987), RothC (Jenkinson et al., 1990) or DAISY (Hansen et al., 1990) model. In these models, soil organic matter (SOM) is typically represented by two or more distinct conceptual C pools, which are characterised by varying rates of first-order decomposition (Yu et al., 2020). In these models, fluxes related to nutrient mineralisation and immobilisation are determined by the efficiency of C transfer between different SOM pools and their specified C-to-N (C: N) stoichiometry (Zhang et al., 2021). While many of the specialised models for soil processes have retained the soil itself as the primary focus of research (soil models), other models have added plant physiological processes (crop models) and have simulated the matter and energy turnover of the entire soil–crop–atmosphere nexus in a balanced manner (agro-ecosystem models; Laniak et al. (2013)). These models play an important role in assessing the consequences of particular management practices, plant characteristics, or environmental variables on agricultural production and its related ecosystem services and disservices (Kirschbaum et al., 2017; Nendel et al., 2014).

Over the last few decades, significant developments have been made in modelling water, C and N fluxes in grassland ecosystems (Huntzinger et al., 2012; Sándor et al., 2016; Warszawski et al., 2014). These studies utilise specialised models tailored to consider a specific range of factors, such as vegetation, soil characteristics, weather conditions, and management strategies that might influence energy and matter exchange within grassland ecosystems (Sándor et al., 2016). Examples have included investigating C cycling in and N leaching from grasslands under various management practices using the DayCent model (Parton et al., 1994), simulating GHG emissions from grazed grasslands using the grassland-specific PaSim model (Riedo et al., 1998), or more broadly investigating feedback regulations in grassland systems under a wide range of management activities and environmental conditions using the STICS model (Brisson et al., 1998). However, none of the existing grassland modelling studies have addressed the interplay of water, C and N cycles in light of fluctuating groundwater tables.

There are still many inconsistencies and gaps in our knowledge of how water, C and N interact in grassland ecosystems, as well as the mechanisms that regulate these interactions (Fatichi and Pappas, 2017; Jung et al., 2017; Katul et al., 2012). As a result, the models used to simulate these interactions are characterised by substantial uncertainties at all scales (Sándor et al., 2017; Van Oijen et al., 2020). This holds especially true for wet grasslands, where the shallow water table causes intensive turnover of water, C and N (Chen et al., 2019; Frolking et al., 2011; Waddington and Price, 2000). In such situations, the resulting fluxes may exhibit high spatial and temporal variability when site conditions are heterogeneous and groundwater levels fluctuate (Frolking et al., 2011). In the context of climate change mitigation, drained wetlands, including bogs and fens, can serve as C sinks after being rewetted and returned to their original state (Günther et al., 2020).

Nevertheless, using mechanistic simulation models to predict the potential sink strength of wet grasslands requires two important functionalities: First, they need to be capable of capturing the response of SOM turnover to the absence of oxygen that occurs under saturated

conditions. Second, they need to reproduce the resumption of decomposition when oxygen becomes available again, e.g. as a result of drainage or evaporation. The MModel for Nitrogen and Carbon dynamics in Agroecosystems (MONICA; [Nendel et al., 2011](#)) is one model that is indeed capable of simulating such a response ([Khaledi et al., 2024](#)). Before using the model for climate change impact assessments and mitigation scenarios for wet grasslands in future studies, our primary objective here is to demonstrate that MONICA is able to simulate interactions between water, C and N fluxes, and the produced GHG emission in a typical wet grassland ecosystem – including its characteristic fluctuating water table depth (WTD). Water, C and N observations for this demonstration (including gas flux measurements, nitrate concentration measurements in the soil solution, and biomass cuts) were obtained from a grassland lysimeter station with controllable water tables. It was against this data that we tested the model.

## 2. Materials and methods

### 2.1. Study site and lysimeter management

The experimental dataset was obtained from an advanced weighable groundwater lysimeter station equipped with chamber system for gas flux measurements. The station, established in 2009, is located in the

Spreewald wetlands of Germany (51°52'N, 14°02'E, [Fig. 1](#); [Dietrich et al., 2016](#)). Four cylindrical soil monoliths, each with a surface area of 1 m<sup>2</sup>, a depth of 2 m, and an existing permanent grassland vegetation cover were placed in the lysimeters in such a way that the soil profile was not disturbed. Dominant species in grass cover were *Carex acuta*, *Festuca arundinacea*, *Festuca rubra*, *Holcus lanatus*, *Plantago lanceolata*, and *Poa pratensis*. Each lysimeter contains a different soil type (Table S1 in the Supplementary Material). The station recorded meteorological conditions (Table S2) including net radiation (CNR 4, Kipp & Zonen), soil heat flux (HFP01SC, Huxeflux), air temperature, relative humidity 2 m above the surface (PC-ME, Galltec + mela), wind speed and wind direction (classic, Thies) ([Dietrich et al., 2016](#)). In addition, a precipitation gauge (Hellmann RG 50, Thies) was positioned at a height of 1 m above the ground. All data has been aggregated to daily values to meet the requirements of the model. The lysimeters were fenced in to protect against animal incursions, and were not additionally fertilised. A detailed description of the technical equipment at the lysimeter station, the associated weather station, data acquisition and data evaluation can be found in [Dietrich et al. \(2016\)](#).

WTD was measured daily in each lysimeter. Unlike conventional groundwater lysimeters that maintain a constant WTD by controlling inflow and outflow, this station used an automatic WTD control system, allowing natural WTD cycles and their impact on water chemistry and

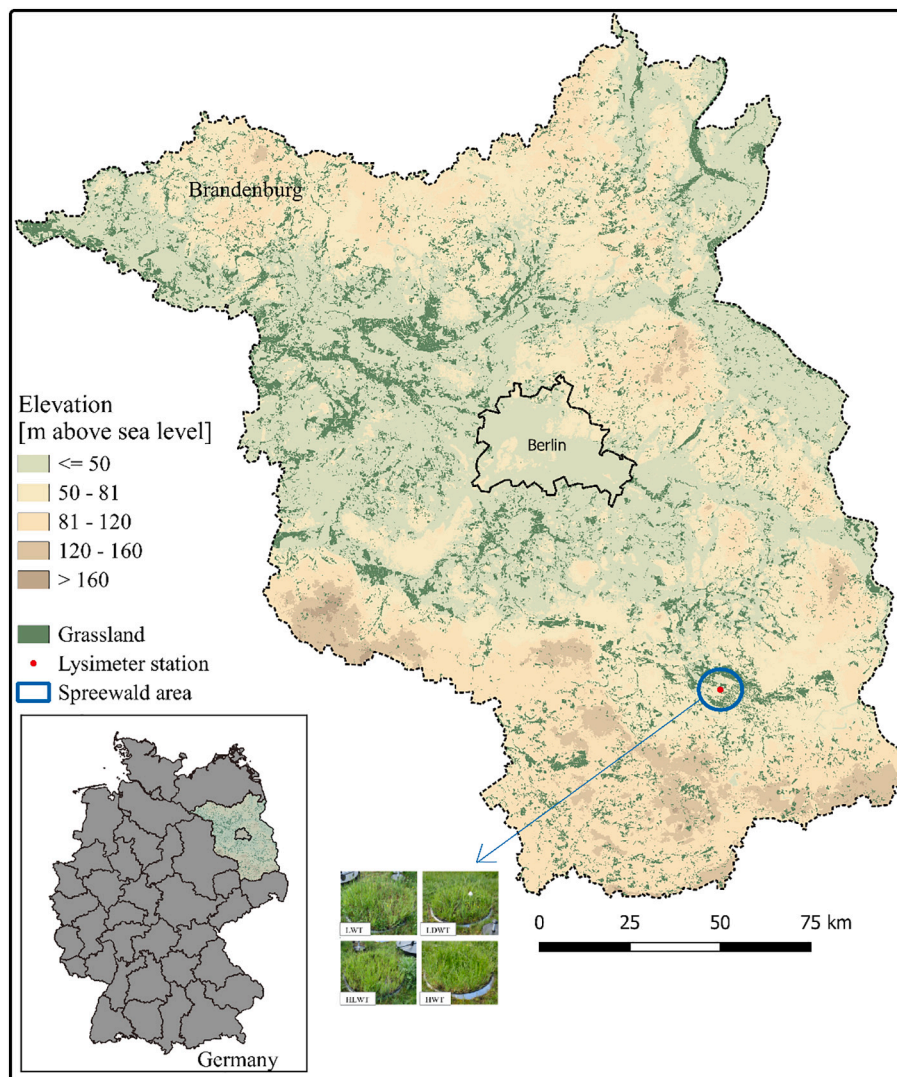


**Fig. 1.** Location of the lysimeter station within the Spreewald wetlands. Grassland areas are highlighted in dark green colour in an elevation map of the Federal State of Brandenburg, Germany.

vegetation to be studied. Two different groundwater treatments were applied in 2021, leading to low variation in biogeochemical processes and related GHG and water fluxes; in 2022, four treatments were applied to trigger greater variation (Table 1). Lysimeter 1 maintained a groundwater level equal to the local conditions for 24 months (2021, 2022; Local Water Table LWT). In Lysimeter 2, the local ground water table was maintained for 12 months, then a water table of 50 cm below the local conditions was set for the following 12 months (Local + Dry Water Table LDWT). Lysimeter 3 and Lysimeter 4 treatments involved water levels exceeding the soil surface by 4 cm, with L4 experiencing flooded conditions for 24 months (High Water Table HWT) and L3 for 18 months, followed by 6 months at the local ground water table (High + Local Water Table HLWT) (Table 1).

With the four different water regimes and soil types, each of the lysimeters presented a unique setting, which was not replicated in the design of the station. From the modelling perspective, any model must be capable in reproducing the target variables in all soil moisture  $\times$  soil type combinations, and the four lysimeters represent samples out this pool of possible combinations. We may assume that the error in reproducing the target variables was similar to the error that the model has produced in previous analyses (e.g. Specka et al., 2016), and that the measurement errors were similar to other lysimeter studies of this kind (Dietrich, 2023; Forstner et al., 2021).

### 2.1.1. Evapotranspiration

In all four lysimeters, the first step was to determine the water balance components. The volume of inflow and outflow was calculated from the hourly change in water level in a compensation tank. We then calculated actual evapotranspiration from the water balance as the difference in total soil core mass between observations (Eq. (1)):

$$ET_a = P - \Delta S + R_{in} - R_{out} \quad (1)$$

where  $ET_a$  is the actual evapotranspiration,  $P$  the precipitation input,  $\Delta S$  the change in soil core mass,  $R_{in}$  the inflow into the lysimeter from the compensation tank and  $R_{out}$  the outflow from the lysimeter into the compensation tank.

An overview of the water table and actual evapotranspiration dynamics throughout the study period is presented in Fig. 2. It includes the potential evapotranspiration ( $ET_p$ ) for reference (Allen et al., 1998). In the first year, the  $ET_a$  of all lysimeters was lower than their  $ET_p$  in all months except for August. Also, in July 2021, the  $ET_a$  of Lysimeter LDWT and Lysimeter HWT was the same as their  $ET_p$ . In 2022, the  $ET_a$  of LWT and HWT was higher than their  $ET_p$  in the same months. In LWT, the  $ET_a$  was significantly higher than its  $ET_p$  in May, due to extensive growth of deep-rooting red clover in that lysimeter. Generally, the year 2021 was wetter and colder than 2022 (Fig. 2).

### 2.1.2. Aboveground biomass

Mowing occurred twice within the growing season, generally in mid-June and early September. Fresh and dry aboveground biomass (AGB) measurements were taken after each mowing event (Dietrich et al., 2021). Results are later reported as dry matter in [ $t \text{ ha}^{-1}$ ]. Prior to the first cut each year, we conducted a vegetation composition assessment

using Mühlenberg (1989) version of the Braun-Blanquet approach, which employs an extended rating scale. This method assesses changes in vegetation by considering species frequency and a range of vegetation indicators, as detailed in (Ellenberg and Leuschner, 2010). The appearance and domination of *Trifolium pratense* (red clover) in LWT during 2022 required serious attention, due to the special characteristics of this species. With its ability to fix N from the atmosphere through Rhizobium bacteria in the root nodules, and its deep-reaching root system (Kutschera et al., 1982), red clover finds optimum growing conditions in LWT and produces much higher biomass than any other species present; this is accompanied by significantly higher transpiration rates.

### 2.1.3. CO<sub>2</sub> flux measurement

Fluxes of CO<sub>2</sub> were measured using a dynamic flow-through non-steady-state closed chamber system with both opaque (ecosystem respiration ( $R_{eco}$ ) flux measurements) and transparent chambers (NEE (net ecosystem exchange) flux measurements; Livingston and Hutchinson, 1995). To measure CO<sub>2</sub> exchange over chamber deployment time (4 min), we connected an infrared gas analyser (LI-850, LI-COR Biosciences, Lincoln, USA) to a data logging unit. During each 4 min of chamber measurement, the CO<sub>2</sub> concentration change in chamber headspace was measured in a frequency of 3 s. CO<sub>2</sub> fluxes were subsequently calculated according to the ideal gas equation (Eq. (2)) as:

$$F = \frac{pV}{RTA} \frac{dc}{dt} \quad (2)$$

where  $F$  denotes the CO<sub>2</sub> flux [ $\text{mol m}^{-2} \text{ s}^{-1}$ ],  $p$  denotes the ambient air pressure [Pa],  $V$  is the chamber volume [ $\text{m}^3$ ],  $R$  refers to the gas constant [ $8.314 \text{ m}^3 \text{ J K}^{-1} \text{ mol}^{-1}$ ],  $T$  denotes chamber air temperature [K],  $A$  is the basal area [ $\text{m}^2$ ] and  $dc \text{ dt}^{-1}$  is the assumed linear CO<sub>2</sub> concentration change in chamber headspace over time in [ $\text{mol mol}^{-1} \text{ s}^{-1}$ ].  $dc/dt$  was determined by applying a linear regressions to multiple data subsets generated by a variable moving window with a minimum length of 30 s (10 consecutive data points). Thus, multiple fluxes per flux measurement were obtained and further on reduced using a list of quality criteria: (i) fulfilled prerequisites for applying a linear regression (normality, variance homogeneity, linearity); (ii) temperature variation within data subset  $< \pm 1.5 \text{ K}$  ( $R_{eco}$  and NEE flux measurements); (iii) PAR variation within data subset  $< \pm 20 \%$  (NEE). Calculated multiple fluxes per measurement that did not meet all quality criteria were discarded. The Flux measurements were conducted twice a month during the growing season and on average once a month during the off-season in both 2021 and 2022. Throughout every campaign, 20–25 measurements were conducted within a span of 1–2 predominantly sunny days (from early morning to late afternoon) to encompass the full spectrum of air and soil temperatures as well as photosynthetic active radiation. The measured CO<sub>2</sub> fluxes were separated into their respective flux components – the  $R_{eco}$  as the sum of the respired CO<sub>2</sub> from the soil organisms and the plant, and the gross primary productivity (GPP) as the rate at which vegetation captures CO<sub>2</sub> in its biomass through photosynthesis (Hoffmann et al., 2015; Hoffmann et al., 2017). To obtain daily NEE,  $R_{eco}$  and GPP fluxes, a flux separation was performed following Hoffmann et al. (2015); Hoffmann et al. (2018), using empirically derived

**Table 1**  
Water table management in the lysimeters.

Lysimeter	2021		2022	
	Jan – Jun	Jul – Dec	Jan – Jun	Jul – Dec
LWT	Local water table depth		Local water table depth	
LDWT	Local water table depth		Deep water table	
HLWT	Water table above surface		Water table above surface	Local water table depth
HWT	Water table above surface		Water table above surface	

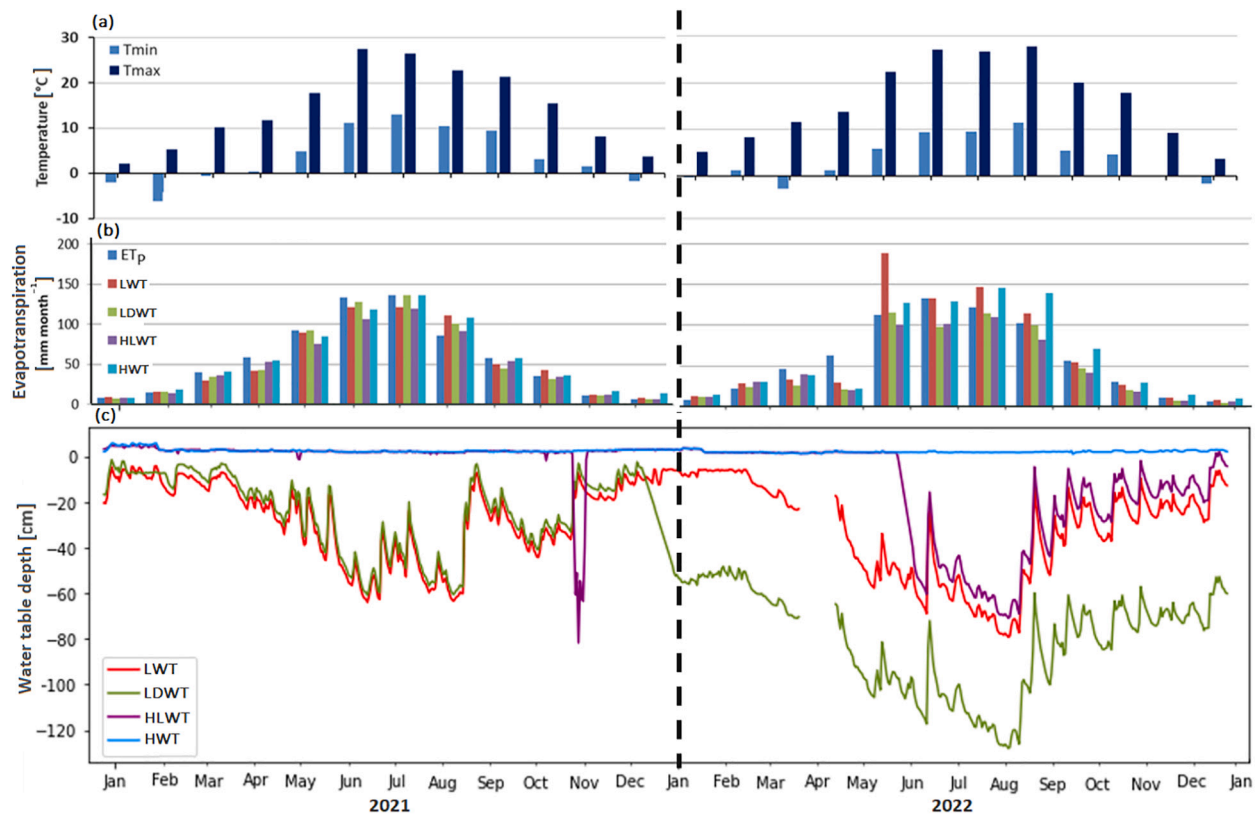


**Fig. 2.** An overview of (a) the daily average of minimum air temperature ( $T_{\min}$ ) and maximum air temperature ( $T_{\max}$ ) for each month, (b) measured actual evapotranspiration ( $ET_a$ ) (note a 20-day data gap in April 2022) and calculated potential evapotranspiration ( $ET_p$ ), and (c) the observed water table depth dynamics in 2021 and 2022 for the four lysimeters LWT (local water table), LDWT (local and dry water table), HLWT (high and local water table) and HWT (high water table).

temperature ( $R_{\text{eco}}$ ; Lloyd and Taylor (1994)) and PAR (GPP; Gilmanov et al. (2013); Moffat et al. (2007)) dependency functions. In case of  $R_{\text{eco}}$ , measured  $R_{\text{eco}}$  fluxes were fitted against measured air and soil temperatures using an Arrhenius type model (Lloyd and Taylor, 1994). Thus,  $R_{\text{eco}}$  parameters, describing the temperature dependency of the measured  $R_{\text{eco}}$  fluxes, were derived for each measurement day. As suggested by Huth et al. (2017), GPP fluxes (for measured NEE fluxes) were subsequently calculated indirectly by subtracting  $R_{\text{eco}}$  fluxes calculated for measured NEE fluxes using derived  $R_{\text{eco}}$  parameters and temperatures measured during transparent chamber measurements. Thus obtained GPP fluxes were fitted against measured PAR using a non-rectangular hyperbolic light response function. Finally campaign-wise daily  $R_{\text{eco}}$ , GPP and NEE fluxes were obtained using derived  $R_{\text{eco}}$  and GPP parameters to calculate and sum half-hourly  $R_{\text{eco}}$ , GPP and NEE fluxes per measurement day.

#### 2.1.4. Nitrogen content measurement

Grassland soils contain pools of inorganic N (nitrate and/or ammonia) derived from various sources. The lysimeter station that we used was fenced in, preventing animals from entering the area. Consequently, there was no significant decomposition of animal waste. There was also no N from fertilisation, as we did not apply fertiliser. As a result, N was primarily produced through the decomposition of plant residues. In addition, we observed the symbiotic fixation effect of red clover in one of the lysimeters in 2022. The N that was not taken up by plants and was lost as a result of the denitrification process ( $N_2$ ,  $N_2O$ ) or by N leaching (nitrification) was measured at the lysimeter station; the amount of N produced through biomass was measured in the lab after each cutting, using a TruSpec CNS elementary analyser (Leco Instruments GmbH) with dried and ground plant material.

**2.1.4.1. Nitrous oxide flux measurement.** To measure Nitrous oxide

( $N_2O$ ), non-flow-through a non-steady-state (NFT-NSS) cylinder-shaped, opaque chamber was used (Livingston and Hutchinson, 1995). The chamber was equipped with a vent on the top to connect beforehand-evacuated glass vials (60 ml) for taking air samples. Glass vials were regularly checked for air storage capabilities using calibration gasses and showed no change in analysed gas concentration for at least two weeks (Loftfield et al., 1997). The first sample of each measurement was taken directly after chamber placement as a zero measurement and was followed by four more samples every 5 min resulting in a total measurement time of 20 min. Air filled glass vials were subsequently analysed for the respective  $N_2O$  gas concentration the week after sampling using a gas chromatograph at ZALF (GC-14A and GC-14B, Shimadzu Scientific Instruments, Japan) equipped with an electron capture detector (ECD) for  $N_2O$  analyses. The ECD operated under a temperature of 280 °C and used pure N as a carrier gas to determine  $N_2O$  concentration from the sampled glass vials (Loftfield et al., 1997).

**2.1.4.2. Nitrate concentration measurement.** Inside each lysimeter, three ceramic suction probes of 20 mm diameter, with an acrylic glass standpipe as a collecting space (Umwelt-Geräte-Technik, 1992), were installed at different depths (30 cm, 60 cm and 90 cm) for soil water extraction, thus providing three samples per lysimeter. We investigated the  $NO_3^-$  in the soil water extracted from the lysimeters in the laboratory. Sampling frequency was fortnightly within the vegetation period, or else every 4 weeks.

## 2.2. The structure of the model

MONICA (Version 3.3.1; Aiteew et al. (2024); Nendel et al. (2011)) is a process-based agroecosystem model simulating crop growth as well as the corresponding water, C and N dynamics for soil–crop–atmosphere systems in a daily time step. MONICA allows to parametrise a soil profile

up to a maximum depth of 2 m, with 10 cm intervals. Soil water dynamics in MONICA is simulated using a capacity approach, including capacity parameters derived from soil texture classes (Eckelmann et al., 2005). While the capacity approach only allows a model to simulate the downward movement of water, MONICA uses an empirical approach that calculates ascending water in the capillary fringe above the water table (Khaledi et al., 2024), employing daily rise rates from the German soil survey manual (Eckelmann et al., 2005). The calculation of  $ET_p$  follows the Penman–Monteith approach (Allen et al., 1998), which involves the use of crop-specific factors ( $K_c$ ) for particular crops and their phenological stages throughout the growing season, and bare-soil factors during the period between harvest and crop emergence (Nendel et al., 2011).

Organic matter turnover is calculated based on routines from the DAISY (Danish Agricultural and Interdisciplinary Simulation System) agro-ecosystem model (Hansen et al., 1990), in which C dynamics is described via three pairs (slow and fast decomposition) of conceptual pools, including added organic matter (AOM), soil microbial biomass (SMB) and soil organic matter (SOM) (Abrahamsen and Hansen, 2000). Decomposition rates, influenced by temperature and moisture, mirror the environmental conditions of the simulated site. The clay content of the soil further affects the rates of decay and respiration in soil microbial biomass. Information about crop residues, provided by MONICA's crop module, is used in the mineralisation routine, where the residue amount and total N content together help determine the C/N ratio (Jensen et al., 2005). MONICA's ability to accurately reproduce the short-term  $CO_2$  exchange and long-term dynamics of C in agricultural soils has been intensively tested by Specka et al. (2016), Farina et al. (2021) and Aiteew et al. (2024).

### 2.2.1. Model calibration

The simulation setup for all lysimeter treatments used crop

parameters for ryegrass (Kamali et al., 2022), except for LWT in the second year. Due to the appearance and rapid domination of red clover, simulations for this lysimeter needed to utilise the parameter set for clover grass, which is characterised by a greater rooting depth and higher levels of biological N fixation. The following observed variables were available for the calibration process: ET, AGB, GPP,  $R_{eco}$ , N in AGB,  $NO_3^-$  leaching and  $N_2O$  production. The study period spanned from 2021 to 2022. However, to convey the fact that sowing was not initiated in 2021, we also incorporated the two years preceding 2021 as a backup period. Therefore, the model setup was based on site information from 2019 to 2022, but the simulation in this study focused solely on the years 2021 and 2022.

### 2.2.2. Parameter selection

An important step in the calibration process was to select the parameters for each specific variable. We classified the parameter selection into four categories: the first group includes the parameters for calibrating the ET simulations, the second group for calibrating AGB simulations, the third for calibrating GPP and  $R_{eco}$ , and the fourth for calibrating N in biomass,  $NO_3^-$  and  $N_2O$  simulations (Table 2). To calibrate ET, we conducted a manual sensitivity analysis and subsequently selected the crop coefficient  $K_c$  as a relevant parameter. The AGB parameter set was taken from Kamali et al. (2022) for intensively used grasslands. The GPP and  $R_{eco}$  parameters were identified from a local sensitivity analysis. For the parameters of the N components, we referred to the sensitivity analysis performed by Specka et al. (2015).

### 2.2.3. SPOTPY optimisation using the SCE-UA algorithm

We calibrated MONICA using the Statistical Parameter Optimisation Tool (SPOTPY) Python package (Houska et al., 2015, 2018), employing the shuffled complex evolution algorithm (SCE-UA) (Duan et al., 1993; Duan et al., 1994). The first step was to determine the parameter sets

**Table 2**

The parameters selected to optimise the simulated variables: aboveground biomass (AGB), evapotranspiration (ET), gross primary productivity (GPP), ecosystem respiration ( $R_{eco}$ ), nitrogen content in AGB, nitrate concentration in the soil water ( $NO_3^-$ ) and Nitrous oxide ( $N_2O$ ) gas flux ( $N_2O$ ) simulation results. Stages 1–6 denote the phenological stages defined in MONICA for each individual crop.

Category	Parameter	Description	Unit	Initial values	Optimal values
ET	InitialKcFactor	Initial crop coefficient factor		0.4	0.4
	StageKcFactor	Crop coefficient factor for 6 different stages		[0.46, 0.93, 1.00, 1.00, 0.96, 0.84]	[0.5, 0.93, 1, 1, 0.94, 0.85]
AGB	AssimilatePartitioningCoeff	Assimilate portion assigned for growth at six stages and for four organs	%	Stage1 [0.7, 0.3, 0, 0]	Stage1 [0.61,0.39,0,0]
				Stage2 [0, 0.4, 0.6, 0]	Stage2 [0, 0.48, 0.52, 0]
				Stage3 [0, 0.5, 0.5, 0]	Stage3 [0, 0.42, 0.58,0]
				Stage4 [0, 0.5, 0.5, 0]	Stage4 [0, 0.4,0.6,0]
				Stage5 [0, 0.5, 0.5, 0]	Stage5 [0,0.25,0.7,0.05]
				Stage6 [0,0,0,0]	Stage6 [0,0.01,0.01,0]
	BaseTemperature	Base temperature for growth at six stages		[1, 2, 4, 4, 4, 4]	[0.7,1.2,3.19,3.37,4.1,3.7]
	SpecificLeafArea	Specific leaf area index at six stages	m <sup>2</sup> kg <sup>-1</sup>	[0.002, 0.002, 0.002, 0.002, 0.002, 0.002]	[0.0031, 0.0022, 0.0021, 0.0026, 0.003, 0.0032]
	CuttingDelayDays	Number of delayed days in growth after cutting	day	10	7.89
	MaxAssimilationRate	Maximum assimilation rate	kg CO <sub>2</sub> ha <sup>-1</sup>	15.3	18.5
GPP, Reco	SMB_UtilizationEfficiency	Substrate utilisation efficiency of soil microbes		0.6	0.45
	SOM_FastUtilizationEfficiency	Microbial utilisation efficiency for rapidly decomposing soil organic matter pool		0.8	0.71
	MinimumTemperatureForAssimilation	Minimum temperature for assimilation		8	8
	OptimumTemperatureForAssimilation	Optimum temperature for assimilation		25	27
N in biomass, NO <sub>3</sub> <sup>-</sup> , N <sub>2</sub> O	MaximumTemperatureForAssimilation	Maximum temperature for assimilation		35	34
	NConcentrationB0	Curvature of the critical N concentration curve		0.001	0.001
	NConcentrationPN	Shape factor of the critical N curve		2.6	2.51
	NConcentrationRoot	Initialisation value for root concentration	kg m <sup>-3</sup>	0.02	0.019
	NitriteOxidationRateCoeffStandard	Nitrite oxidation rate coefficient standard	day <sup>-1</sup>	0.2	0.2

and their upper and lower boundaries. These parameters and limits created the parameter space. The measurements served as the target for optimisation. For the parameters, a guess vector was generated and evaluated based on its fit to the target, determined by calculating the root mean square error (RMSE). The goal was to achieve the lowest RMSE. The optimisation algorithm reached convergence when the stopping criteria with the lowest RMSE were met. Finally, after 1100 repetitions, we ultimately employed the combination of parameters that provided the best performance throughout the entire calibration procedure.

2.2.4. Computation of the model performance

We then compared the simulation results against the observed values for the selected variables to evaluate MONICA's performance. The evaluation was conducted separately for each lysimeter and each year. Two indicators were used for this purpose. First, we used the relative root mean square error (rRMSE) based on Bellocchi et al. (2002); Loague and Green (1991) to quantify the difference between individual pairs of simulated and observed values for each variable relative to the mean of the observed values (Eq. (3)). An rRMSE of 0 describes a perfect model. Second, we used the refined version of Willmott's Index of Agreement ( $d_r$ ), based on Willmott et al. (2012), which assesses the statistical covariation between observed and estimated values (Eq. (4)). Willmott's

$d_r$  ranges between 1.0 (perfect model) and  $-1.0$  (poor model).

$$rRMSE = \sqrt{\frac{1/n \sum_{i=1}^n (P_i - O_i)^2}{\sum_{i=2}^n (\bar{O})^2}} \tag{3}$$

$$d_r = \begin{cases} 1 - \frac{\sum_{i=1}^n |P_i - O_i|}{c \sum_{i=1}^n |O_i - \bar{O}|}, & \text{when :} \\ \sum_{i=1}^n |P_i - O_i| \leq c \sum_{i=1}^n |O_i - \bar{O}| \\ \frac{c \sum_{i=1}^n |O_i - \bar{O}|}{\sum_{i=1}^n |P_i - O_i|} - 1, & \text{when :} \\ \sum_{i=1}^n |P_i - O_i| > c \sum_{i=1}^n |O_i - \bar{O}| \end{cases} \tag{4}$$

where  $P_i; i = 1, 2, \dots, n$ , denotes the predictions, with pairwise matching observations  $O_i; i = 1, 2, \dots, n$ ,  $\bar{O}$  stands for the mean of observed values,

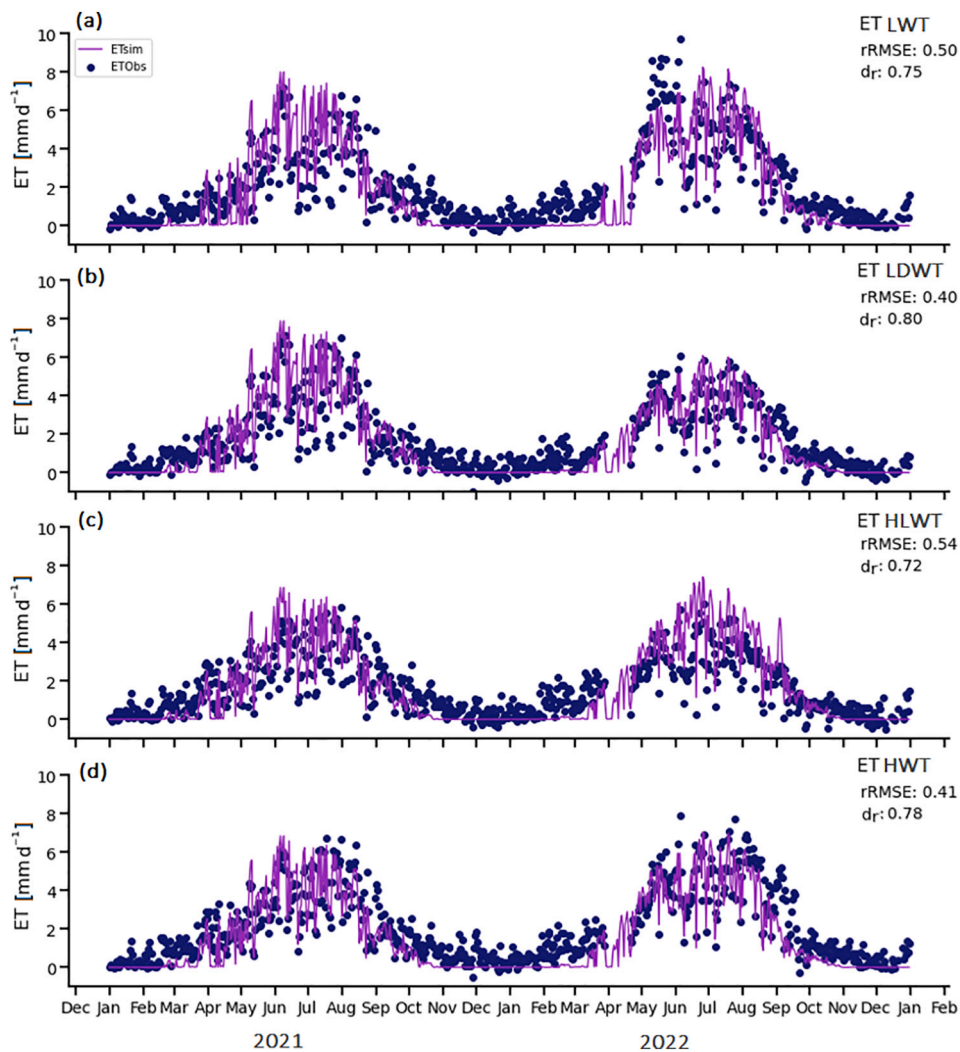


Fig. 3. Simulated (—) versus observed (●) daily evapotranspiration in 2021 and 2022 of the four lysimeters (a) LWT (local water table), (b) LDWT (local and dry water table), (c) HLWT (high and local water table) and (d) HWT (high water table). Model performance indicators: relative root mean square error (rRMSE) and Willmott's refined index of agreement ( $d_r$ ).

and  $c$  represents a constant in the equation ( $c = 2$ ; Willmott et al. (2012)).

### 3. Results

#### 3.1. Evapotranspiration simulation

We assessed the daily simulated ET against the daily observed ET for 2021 and 2022 (Fig. 3). The simulations were slightly better in the second year, with the exception of HLWT, which exhibited overestimation in the second year, and LWT, which demonstrated underestimation. Across the lysimeters, the simulations were always slightly better for LDWT and HWT ( $rRMSE$ : 0.40–0.41;  $d_r$ : 0.80–0.78) than for LWT and HLWT ( $rRMSE$ : 0.50–0.54;  $d_r$ : 0.75–0.72).

#### 3.2. Aboveground biomass and gross primary productivity simulation

Fig. 4 shows the simulation results for AGB and GPP in 2021 and 2022, respectively, alongside the observational values for all lysimeters. The most consistent agreement between observations and AGB simulations was observed for LDWT ( $rRMSE$ : 0.18;  $d_r$ : 0.76) and the least consistent agreement for HWT ( $rRMSE$ : 0.25;  $d_r$ : 0.69); however, this

improved in the second year. While the simulation results for HWT showed improvement in the second year, the simulated AGB peaks for HLWT exhibited a more significant deviation from the observed data points in the second year compared to the first year.

The GPP simulations across all lysimeters demonstrated closer conformity with observations during the second year than during the first year. The  $rRMSE$  ranged between 0.57 and 0.67, and  $d_r$  ranged between 0.62 and 0.69. The expansion of red clover is observed in LWT in the second year through the high amount of AGB production, which was captured by the model by using a specific parameter set for red clover.

#### 3.3. Ecosystem respiration simulation

Fig. 5 shows simulated ecosystem respiration plotted against observed ecosystem respiration.  $rRMSE$  values ranged between 0.54 and 0.68, and  $d_r$  ranged between 0.36 and 0.55, with no notable difference between years and treatments. One notable aspect is that, in some cases, the model did not capture the rapid  $R_{eco}$  recovery in July, after a strong reduction due to the first cut.

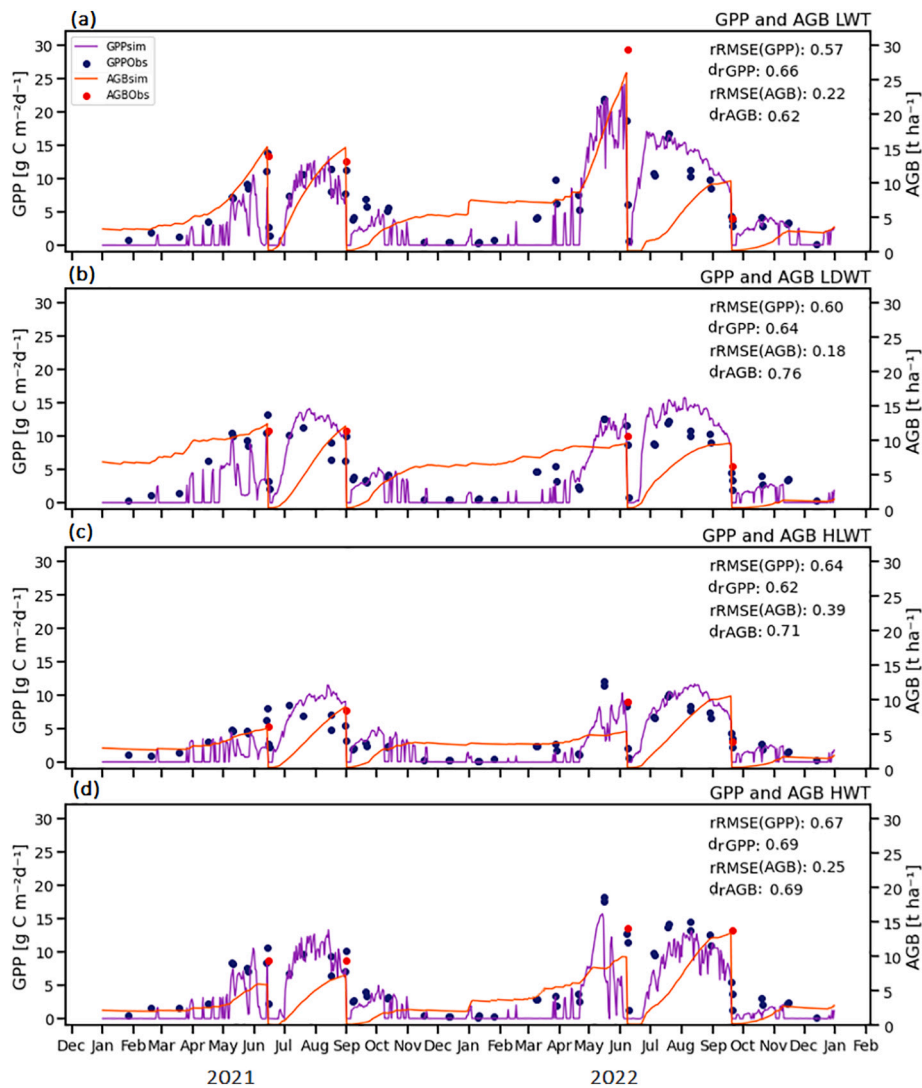
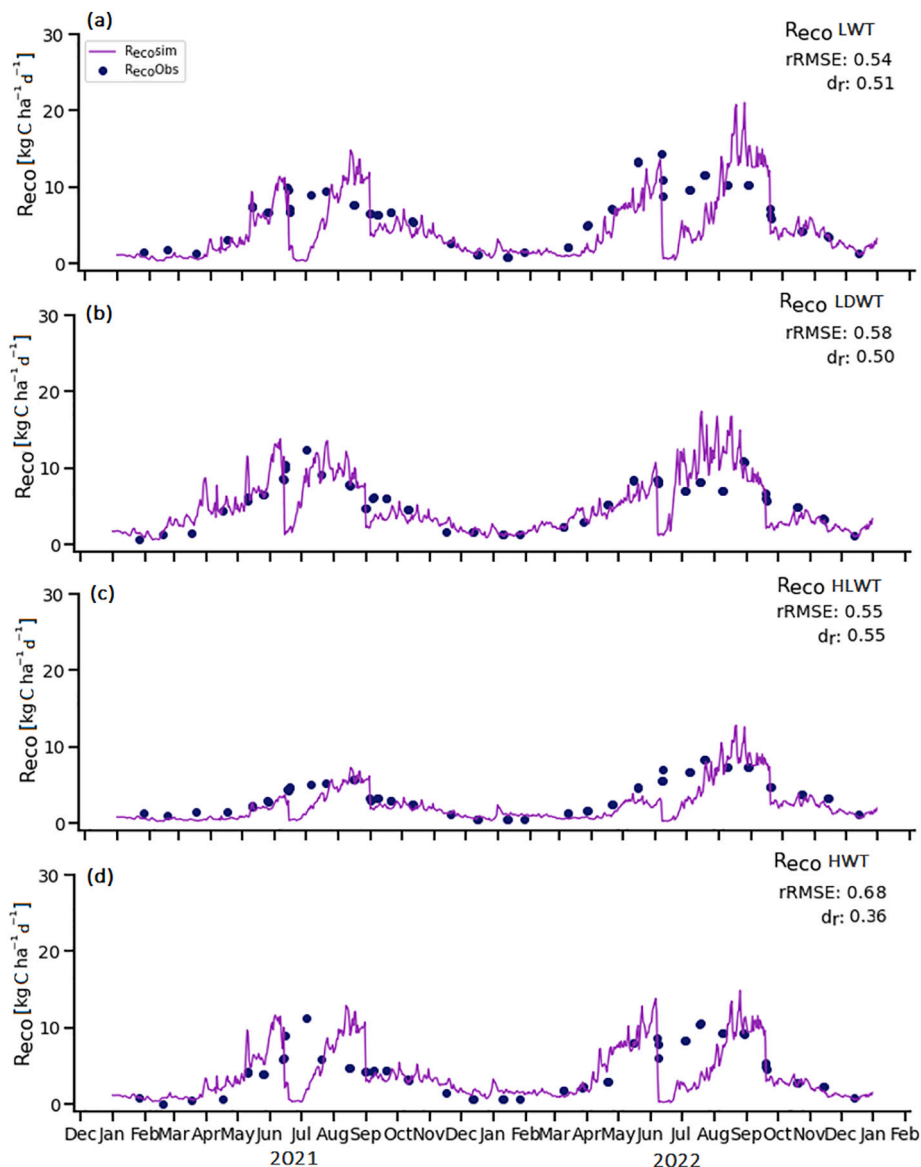


Fig. 4. Simulated (—) versus observed (●) daily aboveground biomass (orange) and gross primary productivity (purple) for 2021 and 2022 of the four lysimeters (a) LWT (local water table), (b) LDWT (local and dry water table), (c) HLWT (high and local water table) and (d) HWT (high water table). Model performance indicators: relative root mean square error ( $rRMSE$ ) and Willmott's refined index of agreement ( $d_r$ ).



**Fig. 5.** Simulated (—) versus observed (●) daily ecosystem respiration, in 2021 and 2022, of the four lysimeters (a) LWT (local water table), (b) LDWT (local and dry water table), (c) HLWT (high and local water table) and (d) HWT (high water table). Model performance indicators: relative root mean square error (rRMSE) and Willmott's refined index of agreement ( $d_r$ ).

### 3.4. Nitrogen in aboveground biomass

Fig. 6 shows the nitrogen content in the AGB plotted against the simulated N in biomass from MONICA. The model captured the N uptake dynamics well in the different lysimeters, ranging from 189 kg N/ha in L1 (first cut, second year) to 24 kg N/ha in LDWT (second cut, second year). rRMSE values ranged between 0.20 and 0.31, and  $d_r$  values ranged between 0.66 and 0.74, with no significant difference between years or lysimeters.

### 3.5. Nitrate concentration simulation

The nitrate concentration in the soil measured at a depth of 30 cm was used in this study to compare it with the nitrate concentrations simulated using MONICA. Since there was no additional N fertiliser added to the lysimeters, the total amount of N cycling in the system and the measured nitrate concentration in soil water extracts from the lysimeters was very low, but the model reproduced this level well (Fig. 7). Due to the consistently low concentrations, the rRMSE values

(0.47–0.57) may potentially misconstrue the model's performance, but the  $d_r$  values (0.44–0.64) nevertheless confirm the strong statistical association between simulations and observations. MONICA not only accurately reproduced the minimal temporal variance, but also depicted the correct nitrate concentration levels. Due to a technical problem with the suction probe in the LDWT lysimeter in the second year, we were only able to secure two measurements.

### 3.6. Nitrous oxide simulation

Similar to  $\text{NO}_3^-$ , the absence of fertilisation meant that the measured quantity of  $\text{N}_2\text{O}$  produced and released into the atmosphere was very small (Fig. 8), including slightly negative fluxes that may occur under waterlogging conditions or in the presence of N-fixing species or simply as a result of the measurement error when values are close to the detection limit (Berendt et al., 2023). This was also accurately reproduced in the simulation. Given that MONICA consistently assumed  $\text{N}_2\text{O}$  to be zero, the rRMSE primarily reflects the proximity of the measured  $\text{N}_2\text{O}$  values to zero. Consequently, for this segment of the simulation, we

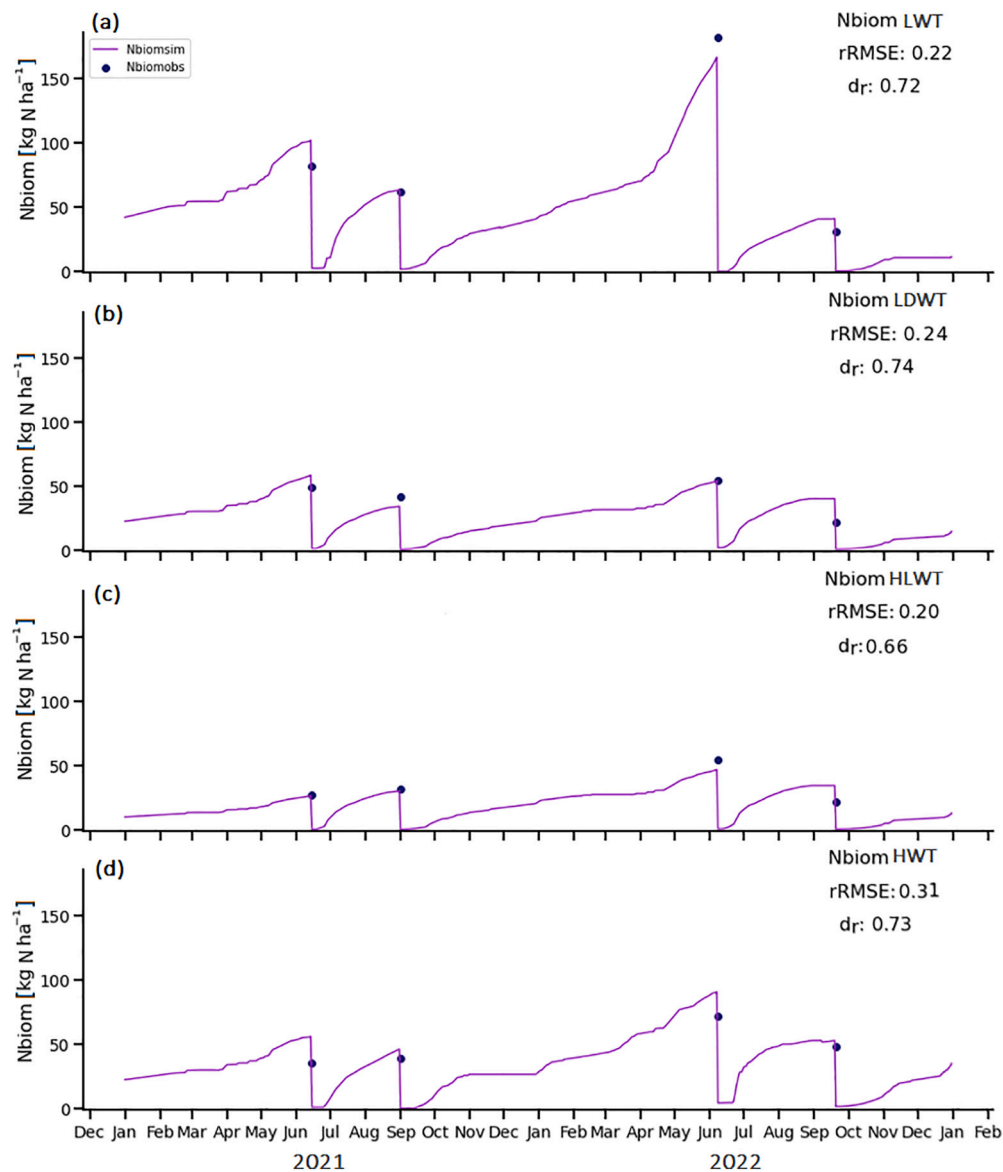


**Fig. 6.** Simulated (—) versus observed (●) daily accumulated nitrogen content in the aboveground biomass (Nbiom) in 2021 and 2022 of the four lysimeters (a) LWT (local water table), (b) LDWT (local and dry water table), (c) HLWT (high and local water table) and (d) HWT (high water table). Model performance indicators: relative root mean square error (rRMSE) and Willmott's refined index of agreement (d<sub>r</sub>).

can infer that MONICA effectively captured the observation that, in the absence of N resources such as fertilisation and without contributions from animals in grasslands, the N<sub>2</sub>O levels would be negligible.

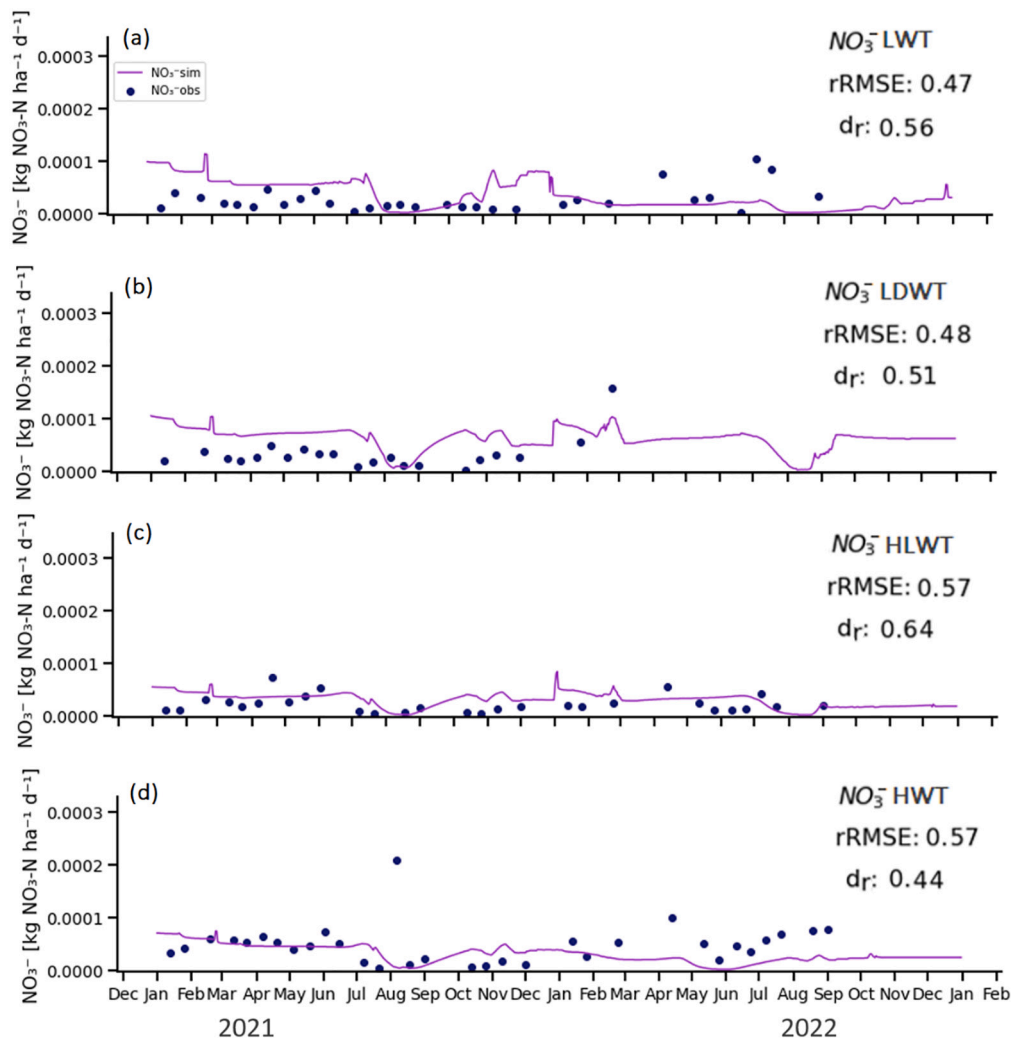
### 3.7. Summary of simulation performance

Table 3 shows the overall comparison of rRMSE for all lysimeters in 2021 and 2022. Across all variables, the simulation showed acceptable and even very good results. While some performance indices suffer from a small number of observations (AGB, N in biomass (Nbiom)), others suggest a low performance rather because they were designed to function with more symmetric error distributions. This precondition was not always met due to the seasonal dynamics that includes periods of very low values where deviations between the simulated and the observed values easily become larger than the average observation in that particular period (ET, GPP, R<sub>eco</sub>). From additional visual inspection, it is also critical to note that both the level and the temporal dynamics of all observed variables was well reproduced by the model.

## 4. Discussion

### 4.1. The lysimeter experiment

Wet grassland ecosystems are inherently complex, given the large range of very different species involved, the fluctuations in water and nutrient availability, and the diverse range of management practices applied. These inherent complexities, together with the direct and indirect effects of climate change, present numerous challenges to modelling the behaviour of the system; researchers have grappled with these challenges for years (Kipling et al., 2016). While simulation model applications to cropping systems can look back on a longer history of success (Bergez et al., 2023), the simulation of temperate grassland systems is not as developed. However, temperate grasslands are responsible for a range of climate-relevant emissions, and can be seen as targetable options for C sequestration (Van Oijen et al., 2020; Yang et al., 2019). In particular, wet grasslands can be very vivid examples of how agricultural management can lead to massive C losses in soils that had been filled with water for millennia before they were drained



**Fig. 7.** Simulated (—) versus observed (●) daily nitrate concentrations ( $\text{NO}_3^-$ ) in the soil water extracts in 2021 and 2022 of the four lysimeters (a) LWT (local water table), (b) LDWT (local and dry water table), (c) HLWT (high and local water table) and (d) HWT (high water table). Model performance indicators: relative root mean square error (rRMSE) and Willmott's refined index of agreement ( $d_r$ ).

(Freeman et al., 2022). Here, field observations and reliable simulations are both urgently lacking; they would underscore the importance of proper management of such systems and could test current rewetting hypotheses.

## 4.2. Model performance

### 4.2.1. Evapotranspiration

Wet grassland sites with a shallow groundwater table usually exhibit different ET patterns compared to other grasslands with a deeper groundwater level (Dietrich and Kaiser., 2017; Huo et al., 2012; Karimov et al., 2014). Simultaneously, studies have found that certain vegetation species transpire significantly more than others (Anda et al., 2014; Dietrich et al., 2021; Queluz et al., 2018; Triana et al., 2015). The MONICA model, employed in simulating ET across all lysimeters, successfully captured the  $\text{ET}_a$  response to changes in the WTD. In the case of the rapid expansion of red clover in LWT during 2022, this required changing the vegetation parameter set to “clover grass” to ensure the proper simulation of this effect. If we had remained with the calibrated parameter set for “grass”, MONICA would have missed this  $\text{ET}_a$  peak. In assessing the model's sensitivity to WTD management, we observed that the model appropriately reflected conditions unfavourable for high ET (e.g. low soil moisture and the absence of plants for transpiration) by simulating accordingly low ET fluxes. This included evaporation from

open water surfaces during periods when the lysimeters were flooded. In general, both the level and the temporal dynamics of  $\text{ET}_a$  were well reproduced by MONICA.

### 4.2.2. Aboveground biomass

AGB exhibits a strong correlation with water availability in the soil (Yinglan et al., 2019). An optimal quantity of water promotes enhanced growth, whereas deviations from this optimum, such as excessive or insufficient water, can have adverse effects (Wan et al., 2022). Even though a range of different optima may exist in a mixed-species community, it was obvious that for the species in HLWT and HWT, supra-optimal amounts of water were present. Consequently, the AGB grown in HLWT and HWT produced lower yields than in the other two lysimeters in the first year. The MONICA model successfully reproduced this pattern, but had notable difficulties in the second year. Another remaining challenge is the change in the species composition as a response to changes in water supply (Khaledi et al., 2024). Here again, as mentioned before for ET, the accurate capture of the significant surge in AGB in LWT caused by the expansion of red clover was only possible by changing the crop parameter sets. There is no automatic routine available in MONICA that would enable the simulation of such a transition, but the tool does include a clover grass setup with existing phenology stages and plant behaviour. Red clover can fix nitrogen from the atmosphere and develop deeper roots compared to the other species

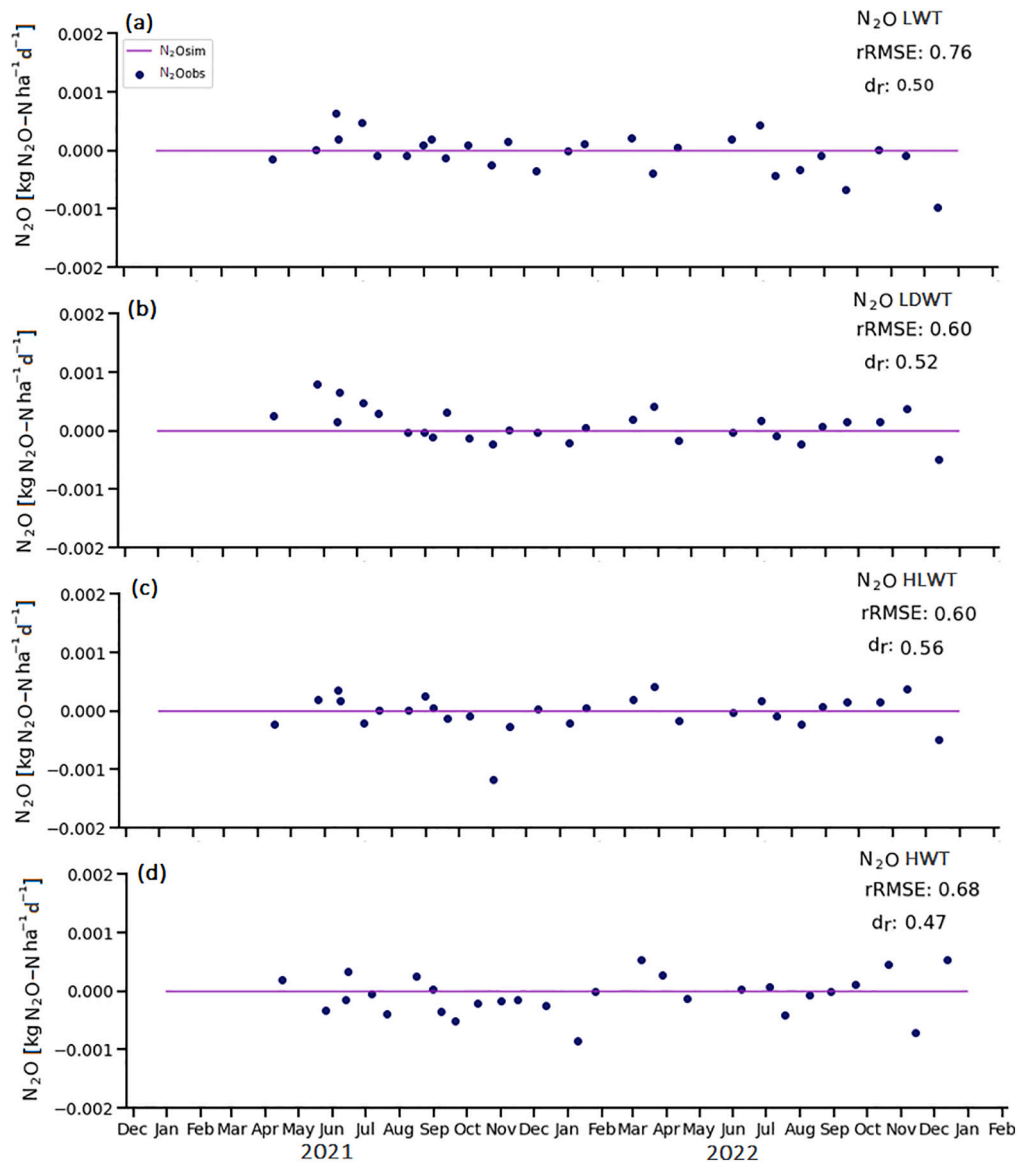


**Fig. 8.** Simulated (—) versus observed (●) daily nitrous oxide (N<sub>2</sub>O) in 2021 and 2022, of the four lysimeters (a) LWT (local water table), (b) LDWT (local and dry water table), (c) HLWT (high and local water table) and (d) HWT (high water table). Model performance indicators: relative root mean square error (rRMSE) and Willmott's refined index of agreement (d<sub>r</sub>).

**Table 3**

Relative root mean square error (rRMSE) and Willmott's refined index of agreement (d<sub>r</sub>) of simulated evapotranspiration (ET), aboveground biomass (AGB), gross primary productivity (GPP), ecosystem respiration (R<sub>eco</sub>), nitrogen in biomass (N<sub>biom</sub>), nitrate concentration in the soil solution (NO<sub>3</sub><sup>-</sup>) and Nitrous oxide (N<sub>2</sub>O) in 2021 and 2022 for the four lysimeter treatments; LWT (local water table), LDWT (local and dry water table), HLWT (high and local water table) and HWT (high water table).

Lysimeter	ET		AGB		GPP		R <sub>eco</sub>		N <sub>biom</sub>		NO <sub>3</sub> <sup>-</sup>		N <sub>2</sub> O	
	rRMSE	d <sub>r</sub>	rRMSE	d <sub>r</sub>	rRMSE	d <sub>r</sub>	rRMSE	d <sub>r</sub>	rRMSE	d <sub>r</sub>	rRMSE	d <sub>r</sub>	rRMSE	d <sub>r</sub>
LWT	0.50	0.75	0.22	0.62	0.57	0.66	0.54	0.51	0.22	0.72	0.47	0.56	0.76	0.50
LDWT	0.40	0.80	0.18	0.76	0.60	0.64	0.58	0.50	0.24	0.74	0.48	0.51	0.60	0.52
HLWT	0.54	0.72	0.39	0.71	0.64	0.62	0.55	0.55	0.20	0.66	0.57	0.64	0.60	0.56
HWT	0.41	0.78	0.19	0.69	0.67	0.69	0.68	0.36	0.31	0.73	0.57	0.44	0.68	0.47

that grow in the lysimeters, and, with better access to nitrogen and water, can produce much higher AGB.

**4.2.3. Gross primary productivity**

The C budget is the foundation for simulations of biomass growth. While AGB is easy to observe, measuring belowground biomass requires

much greater effort and is therefore not a standard observation available for model development, calibration or testing. Belowground biomass was also not available for this study. Instead, our lysimeter experiment delivered CO<sub>2</sub> fluxes into and out of the system, expressed as GPP. GPP in ecosystems serves as a crucial link between soil, plants, atmosphere and the global C cycle (Beer et al., 2010; Liao et al., 2023). Reproducing

GPP and AGB growth at the same time strengthens the assumption that the model simulates biomass correctly on the basis of the C budget (being right for the right reason). In our case, MONICA simulated GPP well, i.e. with a similar error range as compared to the AGB simulations, and with  $d_r$  values well above +0.6 (for  $n = 57$ ). This includes the case of the unusual expansion of red clover observed in LWT, where we equipped MONICA with parameters for clover grass. The increased plant coverage observed with the proliferation of red clover, and a resulting increase in GPP, corresponds to findings by Eckhardt et al. (2018). The increase in both AGB and GPP was successfully reproduced by MONICA for this case.

#### 4.2.4. Ecosystem respiration

Given the proximity of the water table to the surface in wet grasslands, it is imperative that the influence of soil water content as a result of the ground water table distance is considered in the simulation (Bellocchi et al., 2023; Li et al., 2022; Sándor et al., 2016; Smith et al., 2016). Water availability not only governs the growth of vegetation; the level of water that fills the pore space (and displaces oxygen-rich air) also has a major effect on the activity of soil microorganisms and their respiration. Measured ecosystem respiration can act as a lump variable, combining the  $\text{CO}_2$  respiration from vegetation and soil microorganisms. MONICA simulates both processes independently in response to temperature and water availability (or water-filled pore space). Here, the model successfully reproduced the seasonal pattern of  $R_{\text{eco}}$  over the two years, with  $d_r$  values well above 0.35 (for  $n = 57$ ). Even though at  $d_r$  values between 0.0 and 0.5, the observed mean  $\bar{O}$  would become a better predictor, it still indicates that the sum of the prediction error magnitudes is lower than the sum of the perfect-model-deviation and observed-deviation magnitudes (Willmott et al., 2012). Furthermore, against the background that  $\bar{O}$  would be unknown, the model visually captured well the overall dynamics of the target variable. This demonstrates that MONICA indeed added realistic  $\text{CO}_2$  fluxes through respiration to the previously tested  $\text{CO}_2$  fluxes through photosynthesis at the plant level, and also plausible  $\text{CO}_2$  fluxes driven by the respiration of soil microorganisms. This strengthens the hypothesis that MONICA can accurately reproduce the complete C budget of the ecosystem, which makes it appropriate for simulating scenarios of environmental or management impact on the C balance in wet grasslands.

#### 4.2.5. Nitrogen content in biomass

The cycling of N in the soil–plant–atmosphere system is inherently linked to the cycling of C, as both are stoichiometrically bound in organic matter. Now that we have confirmed that the model can cope with C, we can look at the model's performance in simulating N. Simulating the N dynamics accurately has been recognised as a challenge in various modelling studies, in terms of vegetation competition (Faverjon et al., 2019; Grassein et al., 2015) and in terms of soil biology (Hoffmann et al., 2018). To achieve the precise representation of N dynamics in an ecosystem, a process-based model should be capable of simultaneously simulating all N fluxes in the system (Hoffmann et al., 2018). This includes N inputs from fertilisers, the release of N from the turnover of organic matter, and direct N fixation from the air in the roots of legumes, but also N losses through gaseous emissions or leaching.

The easiest to measure and simulate is the N content in AGB, which was well reproduced by MONICA. Again, the red clover expansion in LWT caused a particular challenge, as the plant accumulates much more N in its tissue than the other species in the lysimeter community. The rRMSE for N in biomass prediction in this study aligns with the findings of Dueri et al. (2023), who also used the MONICA model to reproduce N levels in crops.

Lysimeter HLWT in the second year, started out under a wet management regime, and the model showed higher error compared to the first year in the same lysimeter. The model needed an additional year to adjust to the growing and pool-dividing pattern, as observed in HWT. In

HWT, the first year showed higher error compared to the second year, as the model adjusted to the submerged condition, exhibiting an oxygen-deficit signal. Therefore, the lower N content in biomass better aligns with reality after the first year.

#### 4.2.6. Nitrate

In the absence of additional N inputs from animals or fertilisation, nitrate concentrations in the soil remained at notably low levels (Hou et al., 2023). In contrasting cropland environments, where significantly higher concentrations of N occur following high mineral fertiliser additions, MONICA previously demonstrated the ability to reproduce the temporal dynamics of soil mineral nitrogen dynamics (Nendel et al., 2011). Contributing factors, such as the prevalence of shallow-rooted species (Hooper and Vitousek, 1998; Scherer-Lorenzen et al., 2003), as well as considerations of species richness (Leimer et al., 2014), result in diminished downward water flux, consequently reducing nitrate leaching in wet grasslands. The positive correlation observed between water and nutrient availability and plant growth, coupled with increased diversity, contributes to elevated biomass production, ultimately mitigating nitrate losses through leaching (Tilman et al., 1996). In addition, under submerged conditions such as those observed in HLWT during the second year and HWT, limited oxygen availability impeded both soil organic matter (SOM) decomposition and nitrification processes, thereby reducing  $\text{NO}_3^-$  leaching. Notably, the grass species investigated in this study have been noted for their propensity to generate low nitrate leaching during the growing season (Børgesen et al., 2022).

The application of the MONICA model proved successful in accurately reproducing low N levels, facilitated by the concurrent provision of fertilisation information and the meticulous parameterisation; all of this ensured a comprehensive representation of the plant life cycle. The model effectively categorised organic matter pools, accurately attributing them to nitrification and denitrification processes, and thereby corresponding to its commendable overall performance in simultaneously simulating water, C and N content dynamics.

#### 4.2.7. Nitrous oxide

In this study,  $\text{N}_2\text{O}$  simulation was consistently zero throughout the investigation period, as the N input to the lysimeters was solely from plant residues, while high inputs of N fertiliser and other trigger events are missing. The weakest performance of MONICA in simulating  $\text{N}_2\text{O}$  was observed in LWT during the second year, when the expansion of red clover occurred. This led to a higher production of  $\text{N}_2\text{O}$  compared to other lysimeters in different years which the model did not capture. Overall, the measured  $\text{N}_2\text{O}$  fluxes were very low, close to the measurement error of the system. A part of the  $\text{N}_2\text{O}$  produced was even assimilated again by the vegetation, which led to negative fluxes being observed. If much higher concentrations of mineral nitrogen in the soil were present, e.g. added through fertilisation, much higher  $\text{N}_2\text{O}$  levels would have been recorded, as previously shown in many  $\text{N}_2\text{O}$  emission studies (Abalos et al., 2022; Jerray et al., 2024; Olesen et al., 2023). MONICA has previously demonstrated to pick up  $\text{N}_2\text{O}$  emission peaks two orders of magnitude higher under conditions favourable for denitrification (Dueri et al., 2023). In the light of the previous performance, we consider it a very good result that the model predicted no significant  $\text{N}_2\text{O}$  emissions in the present study. At this level, the performance indicators are misleading, as the total scale of possible  $\text{N}_2\text{O}$  emissions has not been observed in this experiment.

## 5. Conclusion

The Spreewald lysimeter station provides an excellent dataset to test process-based models, with varying soil types and comprehensive data on interconnected variables under different groundwater management levels. This is important, as models often provide very good results for a few tested variables, but potentially fail for others that cannot be tested due to a lack of data (Houska et al., 2017; Kersebaum, 2007).

Recognising that water availability is integral to vegetation growth, which, in turn, feeds back into the nutrient cycle, the Spreewald lysimeters allow for holistic model calibration and testing by covering all relevant variables and studying their interconnectedness.

A process-based model, MONICA, has demonstrated its prowess in accurately reproducing key state variables within wet grassland ecosystems and their feedback relationships. This attests to its suitability for simulating environmental and management impacts, particularly those associated with near-surface groundwater changes. MONICA's capabilities extend to encompassing various aspects such as C sequestration (in rewetting scenarios), GHG emissions, nitrate leaching, productive and unproductive water loss, and agronomic productivity. Consequently, the model addresses numerous pressing questions associated with the role of wet grasslands in the future agriculture of temperate Europe. Now that its fitness has been demonstrated, a range of different applications can be envisioned, which include scenarios of future climatic conditions, of groundwater level decline, and of groundwater level control via weir management. Most importantly in the context of the most recent discussion on climate mitigation and the agreed targets on net zero emissions, MONICA is now capable of analysing the C sequestration potential of rewetting previously drained fens and bogs. What sets MONICA apart from specialised grassland models is its ability to simulate both lowland and upland grasslands, as well as cropland. This versatility allows MONICA to cover almost the entire short-term managed agricultural landscape (excluding forests), making it particularly valuable for large-scale assessments.

## Funding

Funding for this research was provided by the Leibniz Centre for Agricultural Landscape Research through its Integrated Priority Project entitled "Water and carbon dynamics in agriculturally used wetlands" (ID 2196).

## CRediT authorship contribution statement

**Valeh Khaledi:** Writing – original draft, Visualization, Validation, Methodology, Investigation, Formal analysis, Conceptualization. **Roland Baatz:** Writing – review & editing, Software, Methodology, Investigation. **Danica Antonijević:** Writing – review & editing, Resources, Data curation. **Mathias Hoffmann:** Writing – review & editing, Resources, Methodology, Data curation. **Ottfried Dietrich:** Writing – review & editing, Methodology, Data curation. **Gunnar Lischeid:** Writing – review & editing, Visualization, Supervision, Investigation, Formal analysis. **Mariel F. Davies:** Resources, Data curation. **Christoph Merz:** Writing – review & editing, Project administration, Funding acquisition, Data curation, Conceptualization. **Claas Nendel:** Writing – review & editing, Validation, Supervision, Software, Methodology, Investigation, Funding acquisition, Conceptualization.

## Declaration of competing interest

The authors declare the following financial interests/personal relationships which may be considered as potential competing interests: Valeh Khaledi reports financial support was provided by Leibniz Centre for Agricultural Landscape Research (ZALF). Danica Antonijević reports financial support was provided by Leibniz Centre for Agricultural Landscape Research (ZALF). Mariel Fiona Davies reports financial support was provided by Leibniz Centre for Agricultural Landscape Research (ZALF).

## Data availability

Data will be made available on request.

## Appendix A. Supplementary data

Supplementary data to this article can be found online at <https://doi.org/10.1016/j.scitotenv.2024.174995>.

## References

- Abalos, D., Recous, S., Butterbach-Bahl, K., De Notaris, C., Rittl, T.F., Topp, C.F., Petersen, S.O., Hansen, S., Bleken, M.A., Rees, R.M., 2022. A review and meta-analysis of mitigation measures for nitrous oxide emissions from crop residues. *Sci. Total Environ.* 828, 154388 <https://doi.org/10.1016/j.scitotenv.2022.154388>.
- Abrahamsen, P., Hansen, S., 2000. Daisy: an open soil-crop-atmosphere system model. *Environ. Model. Softw.* 15 (3), 313–330. [https://doi.org/10.1016/S1364-8152\(00\)00003-7](https://doi.org/10.1016/S1364-8152(00)00003-7).
- Abramoff, R., Xu, X., Hartman, M., O'Brien, S., Feng, W., Davidson, E., Finzi, A., Moorhead, D., Schimel, J., Torn, M., 2018. The millennial model: in search of measurable pools and transformations for modeling soil carbon in the new century. *Biogeochemistry* 137, 51–71. <https://doi.org/10.1007/s10533-017-0409-7>.
- Aiteew, K., Rouhiainen, J., Nendel, C., Dechow, R., 2024. Evaluation and optimisation of the soil carbon turnover routine in the MONICA model (version 3.3.1). *Geosci. Model Dev.* 17, 1349–1385. <https://doi.org/10.5194/gmd-17-1349-2024>.
- Allen, R.G., Pereira, L.S., Raes, D., Smith, M., 1998. Crop evapotranspiration-guidelines for computing crop water requirements-FAO irrigation and drainage paper 56. *FAO, Rome* 300 (9), D05109.
- Anda, A., da Silva, J.A.T., Soos, G., 2014. Evapotranspiration and crop coefficient of common reed at the surroundings of Lake Balaton, Hungary. *Aquat. Bot.* 116, 53–59. <https://doi.org/10.1016/j.aquabot.2014.01.008>.
- Beer, C., Reichstein, M., Tomelleri, E., Ciais, P., Jung, M., Carvalhais, N., Rödenbeck, C., Arain, M.A., Baldocchi, D., Bonan, G.B., 2010. Terrestrial gross carbon dioxide uptake: global distribution and covariation with climate. *Science* 329 (5993), 834–838.
- Bellocchi, G., Acutis, M., Fila, G., Donatelli, M., 2002. An indicator of solar radiation model performance based on a fuzzy expert system. *Agron. J.* 94 (6), 1222–1233.
- Bellocchi, G., Barcza, Z., Hollós, R., Acutis, M., Bottyán, E., Doro, L., Hidy, D., Lellei-Kovács, E., Ma, S., Minet, J., 2023. Sensitivity of simulated soil water content, evapotranspiration, gross primary production and biomass to climate change factors in Euro-Mediterranean grasslands. *Agric. For. Meteorol.* 343, 109778 <https://doi.org/10.1016/j.agrformet.2023.109778>.
- Bengtsson, J., Bullock, J., Ego, B., Everson, C., Everson, T., O'connor, T., O'farrell, P., Smith, H., Lindborg, R., 2019. Grasslands—more important for ecosystem services than you might think. *Ecosphere* 10 (2), e02582. <https://doi.org/10.1002/ecs2.2582>.
- Berendt, J., Jurasinski, G., Wrage-Mönnig, N., 2023. Influence of rewetting on N2O emissions in three different fen types. *Nutr. Cycl. Agroecosyst.* 125 (2), 277–293.
- Bergez, J.E., Constantin, J., Debaeke, P., Martin, R., Raynal, H., Plassin, S., Willaume, M., 2023. Advances in Integrating Different Models Assessing the Impact of Climate Change on Agriculture. Burleigh Dodds Science Publishing. <https://doi.org/10.19103/AS.2022.0115.01>.
- Børgesen, C.D., Pullens, J.W., Zhao, J., Blicher-Mathiesen, G., Sørensen, P., Olesen, J.E., 2022. NLES5—an empirical model for estimating nitrate leaching from the root zone of agricultural land. *Eur. J. Agron.* 134, 126465 <https://doi.org/10.1016/j.eja.2022.126465>.
- Brisson, N., Mary, B., Ripoche, D., Jeuffroy, M.H., Ruget, F., Nicoulaud, B., Gate, P., Devienne-Barret, F., Antonioletti, R., Duru, C., 1998. STICS: a generic model for the simulation of crops and their water and nitrogen balances. I. Theory and parameterization applied to wheat and corn. *Agronomie* 18 (5–6), 311–346. <https://doi.org/10.1051/agro:2001005>.
- Chang, J., Ciais, P., Viovy, N., Vuichard, N., Sultan, B., Soussana, J.F., 2015. The greenhouse gas balance of European grasslands. *Glob. Chang. Biol.* 21 (10), 3748–3761.
- Chen, Y., Uriarte, M., Wright, S.J., Yu, S., 2019. Effects of neighborhood trait composition on tree survival differ between drought and postdrought periods. *Ecology* 100 (9), e02766. <https://doi.org/10.1002/ecy.2766>.
- Cong, W.F., van Ruijven, J., Mommer, L., De Deyn, G.B., Berendse, F., Hoffland, E., 2014. Plant species richness promotes soil carbon and nitrogen stocks in grasslands without legumes. *J. Ecol.* 102 (5), 1163–1170. <https://doi.org/10.1111/1365-2745.12280>.
- Dietrich, O., 2023. Effects of Groundwater Levels and Soil Moisture on the Development of Leaf Area Index and Biomass Yield of Wet Grasslands (Lysimeter Data) [Data Set].
- Dietrich, O., Kaiser, 2017. Impact of groundwater regimes on water balance components of a site with a shallow water table. *Ecohydrology* 10 (6). <https://doi.org/10.1002/eco.1867>.
- Dietrich, O., Steidl, J., Pavlik, D., 2012. The impact of global change on the water balance of large wetlands in the Elbe Lowland. *Reg. Environ. Chang.* 12 (4), 701–713. <https://doi.org/10.1007/s10113-012-0286-5>.
- Dietrich, O., Fahle, M., Seyfarth, M., 2016. Behavior of water balance components at sites with shallow groundwater tables: possibilities and limitations of their simulation using different ways to control weighable groundwater lysimeters. *Agric. Water Manag.* 163, 75–89. <https://doi.org/10.1016/j.agwat.2015.09.005>.
- Dietrich, O., Behrendt, A., Wegehenkel, M., 2021. The water balance of wet grassland sites with shallow water table conditions in the north-eastern German lowlands in extreme dry and wet years. *Water* 13 (16), 2259. <https://doi.org/10.3390/w13162259>.

- Duan, Q., Gupta, V.K., Sorooshian, S., 1993. Shuffled complex evolution approach for effective and efficient global minimization. *J. Optim. Theory Appl.* 76, 501–521. <https://doi.org/10.1007/BF00939380>.
- Duan, Q., Sorooshian, S., Gupta, V.K., 1994. Optimal use of the SCE-UA global optimization method for calibrating watershed models. *J. Hydrol.* 158 (3–4), 265–284. [https://doi.org/10.1016/0022-1694\(94\)90057-4](https://doi.org/10.1016/0022-1694(94)90057-4).
- Dueri, S., Léonard, J., Chlebowska, F., Rosso, P., Berg-Mohnicke, M., Nendel, C., Ehrhardt, F., Martre, P., 2023. Sources of uncertainty in simulating crop N<sub>2</sub>O emissions under contrasting environmental conditions. *Agric. For. Meteorol.* 340, 109619 <https://doi.org/10.1016/j.agrformet.2023.109619>.
- Eckelmann, W., Sponagel, H., Grotenthaler, W., Hartmann, K., Hartwich, R., Janetzko, P., Joisten, H., Kühn, D., Sabel, K., Traidl, R., 2005. *Manual of Soil Mapping (KA5)*, 5th ed.
- Eckhardt, T., Knoblach, C., Kutzbach, L., Simpson, G., Abakumov, E., Pfeiffer, E.-M., 2018. Partitioning CO<sub>2</sub> net ecosystem exchange fluxes on the microsite scale in the Lena River Delta, Siberia. *Biogeosci. Discuss.* <https://doi.org/10.5194/bg-2018-311>.
- Edwards, K.R., Bárta, J., Mastný, J., Píček, T., 2023. Multiple environmental factors, but not nutrient addition, directly affect wet grassland soil microbial community structure: a mesocosm study. *FEMS Microbiol. Ecol.* [fiad070](https://doi.org/10.1093/femsec/fiad070).
- Ellenberg, H., Leuschner, C., 2010. Vegetation of Central Europe With the Alps: From an Ecological, Dynamic and Historical Perspective. <https://doi.org/10.36198/9783825281045>.
- Farina, R., Sándor, R., Abdalla, M., Álvaro-Fuentes, J., Bechini, L., Bolinder, M.A., Brilli, L., Chenu, C., Clivot, H., De Antoni Migliorati, M., 2021. Ensemble modelling, uncertainty and robust predictions of organic carbon in long-term bare-fallow soils. *Glob. Chang. Biol.* 27 (4), 904–928. <https://doi.org/10.1111/gcb.15441>.
- Fatichi, S., Pappas, C., 2017. Constrained variability of modeled T: ET ratio across biomes. *Geophys. Res. Lett.* 44 (13), 6795–6803. <https://doi.org/10.1002/2017GL074041>.
- Fatichi, S., Manzoni, S., Or, D., Paschalis, A., 2019. A mechanistic model of microbially mediated soil biogeochemical processes: a reality check. *Glob. Biogeochem. Cycles* 33 (6), 620–648. <https://doi.org/10.1029/2018GB006077>.
- Faverjon, L., Escobar-Gutiérrez, A., Litrico, I., Julier, B., Louarn, G., 2019. A generic individual-based model can predict yield, nitrogen content, and species abundance in experimental grassland communities. *J. Exp. Bot.* 70 (9), 2491–2504. <https://doi.org/10.1093/jxb/ery323>.
- Forstner, V., Groh, J., Vremec, M., Herndl, M., Vereecken, H., Gerke, H.H., Birk, S., Pütz, T., 2021. Response of water fluxes and biomass production to climate change in permanent grassland soil ecosystems. *Hydrol. Earth Syst. Sci.* 25 (12), 6087–6106.
- Freeman, B.W., Evans, C.D., Musarika, S., Morrison, R., Newman, T.R., Page, S.E., Wiggs, G.F., Bell, N.G., Styles, D., Wen, Y., 2022. Responsible agriculture must adapt to the wetland character of mid-latitude peatlands. *Glob. Chang. Biol.* 28 (12), 3795–3811. <https://doi.org/10.1111/gcb.16152>.
- Frolking, S., Talbot, J., Jones, M.C., Treat, C.C., Kauffman, J.B., Tuittila, E.-S., Roulet, N., 2011. Peatlands in the Earth's 21st century climate system. *Environ. Rev.* 19 (NA), 371–396. <https://doi.org/10.1139/a11-014>.
- Gibson, D.J., Newman, J.A., 2019. *Grasslands and Climate Change*. Cambridge University Press. <https://doi.org/10.1017/9781108163941.003>.
- Gilmanov, T.G., Wylie, B.K., Tieszen, L.L., Meyers, T.P., Baron, V.S., Bernacchi, C.J., Billesbach, D.P., Burba, G.G., Fischer, M.L., Glenn, A.J., 2013. CO<sub>2</sub> uptake and ecophysiological parameters of the grain crops of midcontinent North America: estimates from flux tower measurements. *Agric. Ecosyst. Environ.* 164, 162–175.
- Grassein, F., Lemauiel-Lavent, S., Lavorel, S., Bahn, M., Bardgett, R.D., Desclos-Theveniau, M., Laîné, P., 2015. Relationships between functional traits and inorganic nitrogen acquisition among eight contrasting European grass species. *Ann. Bot.* 115 (1), 107–115. <https://doi.org/10.1093/aob/mcu233>.
- Günther, A., Barthelmes, A., Huth, V., Joosten, H., Jurasinski, G., Koesch, F., Couwenberg, J., 2020. Prompt rewetting of drained peatlands reduces climate warming despite methane emissions. *Nat. Commun.* 11 (1), 1644. <https://doi.org/10.1038/s41467-020-15499-z>.
- Hansen, S., Jensen, H., Nielsen, N., Svendsen, H., 1990. Daisy, a soil plant system model. Danish simulation model for transformation and transport of energy and matter in the soil plant atmosphere system. *Natl. Agency Environ. Prot.* 369.
- Hénin, S., Dupuis, M., 1945. *Essai de Bilan de la Matière Organique du Sol*. Dudod.
- Hoffmann, M., Jurisch, N., Borraz, E.A., Hagemann, U., Dröslner, M., Sommer, M., Augustin, J., 2015. Automated modeling of ecosystem CO<sub>2</sub> fluxes based on periodic closed chamber measurements: a standardized conceptual and practical approach. *Agric. For. Meteorol.* 200, 30–45. <https://doi.org/10.1016/j.agrformet.2014.09.005>.
- Hoffmann, M., Schulz-Hanke, M., Garcia Alba, J., Jurisch, N., Hagemann, U., Sachs, T., Sommer, M., Augustin, J., 2017. A simple calculation algorithm to separate high-resolution CH<sub>4</sub> flux measurements into ebullition- and diffusion-derived components. *Atmos. Meas. Tech.* 10 (1), 109–118. <https://doi.org/10.5194/amt-10-109-2017>.
- Hoffmann, M.P., Isselstein, J., Rötter, R.P., Kayser, M., 2018. Nitrogen management in crop rotations after the break-up of grassland: insights from modelling. *Agric. Ecosyst. Environ.* 259, 28–44. <https://doi.org/10.1016/j.agee.2018.02.009>.
- Hooper, D.U., Vitousek, P.M., 1998. Effects of plant composition and diversity on nutrient cycling. *Ecol. Monogr.* 68 (1), 121–149. [https://doi.org/10.1890/0012-9615\(1998\)068\[0121:EOPCAD\]2.0.CO;2](https://doi.org/10.1890/0012-9615(1998)068[0121:EOPCAD]2.0.CO;2).
- Hou, E., Ma, S., Huang, Y., Zhou, Y., Kim, H.S., López-Blanco, E., Jiang, L., Xia, J., Tao, F., Williams, C., 2023. Across-model spread and shrinking in predicting peatland carbon dynamics under global change. *Glob. Chang. Biol.* 29 (10), 2759–2775. <https://doi.org/10.1111/gcb.16643>.
- Houska, T., Kraft, P., Chamorro-Chavez, A., Breuer, L., 2015. SPOTting model parameters using a ready-made python package. *PLoS One* 10 (12), e0145180. <https://doi.org/10.1371/journal.pone.0145180>.
- Houska, T., Kraus, D., Kiese, R., Breuer, L., 2017. Constraining a complex biogeochemical model for CO<sub>2</sub> and N<sub>2</sub>O emission simulations from various land uses by model–data fusion. *Biogeosciences* 14 (14), 3487–3508. <https://doi.org/10.5194/bg-14-3487-2017>.
- Houska, T., Kraft, P., Chamorro-Chavez, A., Breuer, L., 2018. SPOTPY: a python tool for sensitivity and uncertainty analysis of environmental models. In: *EGU general assembly conference abstracts*, p. 7470.
- Huntzinger, D.N., Post, W.M., Wei, Y., Michalak, A., West, T.O., Jacobson, A., Baker, I., Chen, J.M., Davis, K., Hayes, D., 2012. North American Carbon Program (NACP) regional interim synthesis: terrestrial biospheric model intercomparison. *Ecol. Model.* 232, 144–157. <https://doi.org/10.1016/j.ecolmodel.2012.02.004>.
- Huo, Z., Feng, S., Huang, G., Zheng, Y., Wang, Y., Guo, P., 2012. Effect of groundwater level depth and irrigation amount on water fluxes at the groundwater table and water use of wheat. *Irrig. Drain.* 61 (3), 348–356.
- Huth, V., Vaidya, S., Hoffmann, M., Jurisch, N., Günther, A., Gundlach, L., Hagemann, U., Elsgaard, L., Augustin, J., 2017. Divergent NEE balances from manual-chamber CO<sub>2</sub> fluxes linked to different measurement and gap-filling strategies: a source for uncertainty of estimated terrestrial C sources and sinks? *J. Plant Nutr. Soil Sci.* 180 (3), 302–315.
- Jenkinson, D., Rayner, J., 1977. The turnover of soil organic matter in some of the Rothamsted classical experiments. *Soil Sci.* 123 (5), 298–305. <https://doi.org/10.1097/00010694-197705000-00005>.
- Jenkinson, D., Andrew, S., Lynch, J., Goss, M., Tinker, P., 1990. The turnover of organic matter in soil. *Philos. Trans. R. Soc. B Biol. Sci.* 329 (1255), 361–368.
- Jensen, L.S., Salo, T., Palmason, F., Breland, J.A., Henriksen, T.M., Stenberg, B., Pedersen, A., Lundström, C., Esala, M., 2005. Influence of biochemical quality on C and N mineralisation from a broad variety of plant materials in soil. *Plant Soil* 273, 307–326.
- Jerray, A., Rumpel, C., Le Roux, X., Massad, R., Chabbi, A., 2024. N<sub>2</sub>O emissions from cropland and grassland management systems are determined by soil organic matter quality and soil physical parameters rather than carbon stock and denitrifier abundances. *Soil Biol. Biochem.* 190, 109274 <https://doi.org/10.1016/j.soilbio.2023.109274>.
- Joyce, C.B., Simpson, M., Casanova, M., 2016. Future wet grasslands: ecological implications of climate change. *Ecosyst. Health Sustain.* 2 (9), e01240 <https://doi.org/10.1002/ehs2.1240>.
- Jung, M., Reichstein, M., Schwalm, C.R., Huntingford, C., Sitch, S., Ahlström, A., Arneeth, A., Camps-Valls, G., Ciais, P., Friedlingstein, P., 2017. Compensatory water effects link yearly global land CO<sub>2</sub> sink changes to temperature. *Nature* 541 (7638), 516–520. <https://doi.org/10.1038/nature20780>.
- Kamali, B., Stella, T., Berg-Mohnicke, M., Pickert, J., Groh, J., Nendel, C., 2022. Improving the simulation of permanent grasslands across Germany by using multi-objective uncertainty-based calibration of plant-water dynamics. *Eur. J. Agron.* 134 (126464) <https://doi.org/10.1016/j.eja.2022.126464>.
- Karimov, A.K., Šimůnek, J., Hanjra, M.A., Avliyakov, M., Forkutsa, I., 2014. Effects of the shallow water table on water use of winter wheat and ecosystem health: implications for unlocking the potential of groundwater in the Fergana Valley (Central Asia). *Agric. Water Manag.* 131, 57–69. <https://doi.org/10.1016/j.agwat.2013.09.010>.
- Katul, G.G., Oren, R., Manzoni, S., Higgins, C., Parlange, M.B., 2012. Evapotranspiration: a process driving mass transport and energy exchange in the soil-plant-atmosphere-climate system. *Rev. Geophys.* 50 (3) <https://doi.org/10.1029/2011RG000366>.
- Kersebaum, K.C., 2007. Modelling nitrogen dynamics in soil–crop systems with HERMES. *Nutr. Cycl. Agroecosyst.* 77, 39–52. <https://doi.org/10.1007/s10705-006-9044-8>.
- Khaledi, V., Kamali, B., Lischeid, G., Dietrich, O., Davies, M.F., Nendel, C., 2024. Challenges of including wet grasslands with variable groundwater tables in large-area crop production simulations. *Agriculture* 14 (5), 679. <https://doi.org/10.3390/agriculture14050679>.
- Kipling, R.P., Virkajärvi, P., Breitsameter, L., Curnel, Y., De Swaef, T., Gustavsson, A.-M., Hennart, S., Höglind, M., Järvenranta, K., Minet, J., 2016. Key challenges and priorities for modelling European grasslands under climate change. *Sci. Total Environ.* 566, 851–864. <https://doi.org/10.1016/j.scitotenv.2016.05.144>.
- Kirschbaum, M.U., Schipper, L.A., Mudge, P.L., Rutledge, S., Puche, N.J., Campbell, D.I., 2017. The trade-offs between milk production and soil organic carbon storage in dairy systems under different management and environmental factors. *Sci. Total Environ.* 577, 61–72. <https://doi.org/10.1016/j.scitotenv.2016.10.055>.
- Kutschera, L., Lichtenegger, E., Sobotik, M., 1982. Root atlas of central European grassland plants. Volume I. Monocotyledoneae. In: *Root Atlas of Central European Grassland Plants. Volume I. Monocotyledoneae*.
- Laniak, G.F., Olchin, G., Goodall, J., Voinov, A., Hill, M., Glynn, P., Whelan, G., Geller, G., Quinn, N., Blind, M., 2013. Integrated environmental modeling: a vision and roadmap for the future. *Environ. Model Softw.* 39, 3–23. <https://doi.org/10.1016/j.envsoft.2012.09.006>.
- Leimer, S., Wirth, C., Oelmann, Y., Wilcke, W., 2014. Biodiversity effects on nitrate concentrations in soil solution: a Bayesian model. *Biogeochemistry* 118, 141–157.
- Li, J., Zhang, Q., Li, Y., Liu, Y., Xu, J., Di, H., 2017. Effects of long-term mowing on the fractions and chemical composition of soil organic matter in a semi-arid grassland. *Biogeosciences* 14 (10), 2685–2696. <https://doi.org/10.5194/bg-14-2685-2017>.
- Li, W., Migliavacca, M., Forkel, M., Denissen, J.M., Reichstein, M., Yang, H., Duveiller, G., Weber, U., Orth, R., 2022. Widespread increasing vegetation sensitivity to soil moisture. *Nat. Commun.* 13 (1), 3959. <https://doi.org/10.1038/s41467-022-31667-9>.

- Liao, Z., Zhou, B., Zhu, J., Jia, H., Fei, X., 2023. A critical review of methods, principles and progress for estimating the gross primary productivity of terrestrial ecosystems. *Front. Environ. Sci.* 11, 464. <https://doi.org/10.3389/fenvs.2023.1093095>.
- Livingston, G., Hutchinson, G., 1995. Enclosure-based measurement of trace gas exchange: applications and sources of error. In: Matson, P.A., Harris, R.C. (Eds.), *Biogenic Trace Gases: Measuring Emissions from Soil and Water*. Blackwell Science Ltd., Oxford, UK, pp. 14–51.
- Lloyd, J., Taylor, J., 1994. On the temperature dependence of soil respiration. *Funct. Ecol.* 315–323.
- Loague, K., Green, R.E., 1991. Statistical and graphical methods for evaluating solute transport models: overview and application. *J. Contam. Hydrol.* 7 (1–2), 51–73.
- Lofffield, N., Flessa, H., Augustin, J., Beese, F., 1997. Automated gas chromatographic system for rapid analysis of the atmospheric trace gases methane, carbon dioxide, and nitrous oxide. *J. Environ. Qual.* 26 (2), 560–564.
- Lohse, K.A., Brooks, P.D., McIntosh, J.C., Meixner, T., Huxman, T.E., 2009. Interactions between biogeochemistry and hydrologic systems. *Annu. Rev. Environ. Resour.* 34, 65–96. <https://doi.org/10.1146/annurev.enviro.33.031207.111141>.
- Mayel, S., Jarrah, M., Kuka, K., 2021. How does grassland management affect physical and biochemical properties of temperate grassland soils? A review study. *Grass Forage Sci.* 76 (2), 215–244. <https://doi.org/10.1111/gfs.12512>.
- Mitsch, W.J., Gosselink, J.G., 2015. *Wetlands*. John Wiley & Sons.
- Moffat, A.M., Papale, D., Reichstein, M., Hollinger, D.Y., Richardson, A.D., Barr, A.G., Beckstein, C., Braswell, B.H., Churkina, G., Desai, A.R., 2007. Comprehensive comparison of gap-filling techniques for eddy covariance net carbon fluxes. *Agric. For. Meteorol.* 147 (3–4), 209–232.
- Mühlenberg, M., 1989. *Freilandökologie*. 2. Auflage. UTB Quelle & Meyer, Verlag Heidelberg Heidelberg.
- Nendel, C., Berg, M., Kersebaum, K.C., Mirschel, W., Specka, X., Wegehenkel, M., Wenkel, K.O., Wieland, R., 2011. The MONICA model: testing predictability for crop growth, soil moisture and nitrogen dynamics. *Ecol. Model.* 222 (9), 1614–1625. <https://doi.org/10.1016/j.ecolmodel.2011.02.01>.
- Nendel, C., Kersebaum, K.C., Mirschel, W., Wenkel, K.O., 2014. Testing farm management options as climate change adaptation strategies using the MONICA model. *Eur. J. Agron.* 52, 47–56. <https://doi.org/10.1016/j.eja.2012.09.005>.
- Olesen, J.E., Rees, R.M., Recous, S., Bleken, M.A., Abalos, D., Ahuja, I., Butterbach-Bahl, K., Carozzi, M., De Notaris, C., Ernfors, M., 2023. Challenges of accounting nitrous oxide emissions from agricultural crop residues. *Glob. Chang. Biol.* 29 (24), 6846–6855. <https://doi.org/10.1111/gcb.16962>.
- Oleson, K., Niu, G.Y., Yang, Z.L., Lawrence, D., Thornton, P., Lawrence, P., Stöckli, R., Dickinson, R., Bonan, G., Lewis, S., 2008. Improvements to the community land model and their impact on the hydrological cycle. *J. Geophys. Res. Biogeosci.* 113 (G1) <https://doi.org/10.1029/2007JG000563>.
- Parton, W.J., Schimel, D.S., Cole, C.V., Ojima, D.S., 1987. Analysis of factors controlling soil organic matter levels in Great Plains grasslands. *Soil Sci. Soc. Am. J.* 51 (5), 1173–1179. <https://doi.org/10.2136/sssaj1987.03615995005100050015x>.
- Parton, W.J., Ojima, D.S., Cole, C.V., Schimel, D.S., 1994. A general model for soil organic matter dynamics: sensitivity to litter chemistry, texture and management. In: *Quantitative Modeling of Soil Forming Processes*, 39, pp. 147–167. <https://doi.org/10.2136/SSASPECPUB39.C9>.
- Queluz, J.G.T., Pereira, F.F.S., Sánchez-Román, R.M., 2018. Evapotranspiration and crop coefficient for *Typha latifolia* in constructed wetlands. *Water Qual. Res. J.* 53 (2), 53–60.
- Raich, J.W., Nadelhoffer, K.J., 1989. Belowground carbon allocation in forest ecosystems: global trends. *Ecology* 70 (5), 1346–1354. <https://doi.org/10.2307/1938194>.
- Ramsar Convention Secretariat, 2010. *Designating Ramsar Sites: Strategic Framework and Guidelines for the Future Development of the List of Wetland for International Importance*, 3 ed.
- Riedo, M., Grub, A., Rosset, M., Fuhrer, J., 1998. A pasture simulation model for dry matter production, and fluxes of carbon, nitrogen, water and energy. *Ecol. Model.* 105 (2–3), 141–183. [https://doi.org/10.1016/S0304-3800\(97\)00110-5](https://doi.org/10.1016/S0304-3800(97)00110-5).
- Rodriguez-Iturbe, I., Porporato, A., Laio, F., Ridolfi, L., 2001. Plants in water-controlled ecosystems: active role in hydrologic processes and response to water stress: I. Scope and general outline. *Adv. Water Resour.* 24 (7), 695–705. [https://doi.org/10.1016/S0309-1708\(01\)00004-5](https://doi.org/10.1016/S0309-1708(01)00004-5).
- Sándor, R., Barcza, Z., Hidy, D., Lellei-Kovács, E., Ma, S., Bellocchi, G., 2016. Modelling of grassland fluxes in Europe: evaluation of two biogeochemical models. *Agric. Ecosyst. Environ.* 215, 1–19. <https://doi.org/10.1016/j.agee.2015.09.001>.
- Sándor, R., Barcza, Z., Acutis, M., Doro, L., Hidy, D., Köchy, M., Minet, J., Lellei-Kovács, E., Ma, S., Perego, A., 2017. Multi-model simulation of soil temperature, soil water content and biomass in Euro-Mediterranean grasslands: uncertainties and ensemble performance. *Eur. J. Agron.* 88, 22–40. <https://doi.org/10.1016/j.eja.2016.06.006>.
- Scherer-Lorenzen, M., Palmberg, C., Prinz, A., Schulze, E.-D., 2003. The role of plant diversity and composition for nitrate leaching in grasslands. *Ecology* 84 (6), 1539–1552. [https://doi.org/10.1890/0012-9658\(2003\)084\[1539:TROPDAJ\]2.0.CO;2](https://doi.org/10.1890/0012-9658(2003)084[1539:TROPDAJ]2.0.CO;2).
- Schimel, J., 2013. Microbes and global carbon. *Nat. Clim. Chang.* 3 (10), 867–868. <https://doi.org/10.1038/nclimate2015>.
- Schmidt, M.W., Torn, M.S., Abiven, S., Dittmar, T., Guggenberger, G., Janssens, I.A., Kleber, M., Kögel-Knabner, I., Lehmann, J., Manning, D.A., 2011. Persistence of soil organic matter as an ecosystem property. *Nature* 478 (7367), 49–56. <https://doi.org/10.1038/nature10386>.
- Smith, K.W., Reed, S.C., Cleveland, C.C., Ballantyne, A.P., Anderegg, W.R., Wieder, W.R., Liu, Y.Y., Running, S.W., 2016. Large divergence of satellite and Earth system model estimates of global terrestrial CO<sub>2</sub> fertilization. *Nat. Clim. Chang.* 6 (3), 306–310. <https://doi.org/10.1038/nclimate2879>.
- Specka, X., Nendel, C., Wieland, R., 2015. Analysing the parameter sensitivity of the agro-ecosystem model MONICA for different crops. *Eur. J. Agron.* 71, 73–87. <https://doi.org/10.1016/j.eja.2015.08.004>.
- Specka, X., Nendel, C., Hagemann, U., Pohl, M., Hoffmann, M., Barkusky, D., Augustin, J., Sommer, M., Van Oost, K., 2016. Reproducing CO<sub>2</sub> exchange rates of a crop rotation at contrasting terrain positions using two different modelling approaches. *Soil Tillage Res.* 156, 219–229. <https://doi.org/10.1016/j.still.2015.05.007>.
- Tilman, D., Wedin, D., Knops, J., 1996. Productivity and sustainability influenced by biodiversity in grassland ecosystems. *Nature* 379 (6567), 718–720. <https://doi.org/10.1038/379718a0>.
- Triana, F., Nasso, N., Ragolini, G., Roncucci, N., Bonari, E., 2015. Evapotranspiration, crop coefficient and water use efficiency of giant reed (*Arundo donax* L.) and miscanthus (*Miscanthus × giganteus* Greef et Deu.) in a Mediterranean environment. *GCB Bioenergy* 7 (4), 811–819.
- Trumbore, S.E., Czimczik, C.I., 2008. An uncertain future for soil carbon. *Science* 321 (5895), 1455–1456. <https://doi.org/10.1126/science.1160232>.
- Umwelt-Geräte-Technik, 1992. UGT GmbH The Solutionists GmbH. <https://ugt-online.de/en/products/soil/suction-probes/>.
- UNFCCC, 2015. Paris Agreement. Report of the Conference of the Parties to the United Nations Framework Convention on Climate Change (21st Session, 2015: Paris) (Retrieved December).
- UNFCCC, 2022. The clean development mechanism (CDM) methodology booklet. In: *United Nations Framework Convention on Climate Change, the Kyoto Protocol and the Paris Agreement, fourteenth ed.*
- Van Oijen, M., Barcza, Z., Confalonieri, R., Korhonen, P., Kröel-Dulay, G., Lellei-Kovács, E., Louarn, G., Louault, F., Martin, R., Moulin, T., 2020. Incorporating biodiversity into biogeochemistry models to improve prediction of ecosystem services in temperate grasslands: review and roadmap. *Agronomy* 10 (2), 259. <https://doi.org/10.3390/agronomy10020259>.
- Waddington, J., Price, J., 2000. Effect of peatland drainage, harvesting, and restoration on atmospheric water and carbon exchange. *Phys. Geogr.* 21 (5), 433–451. <https://doi.org/10.1080/02723646.2000.10642719>.
- Wan, Z., Gu, R., Yan, Y., Bai, L., Bao, T., Yang, J., Gao, Q., Ganjurjav, H., Hu, G., Zhou, H., 2022. Effects of water levels on plant traits and nitrogen use efficiency in monoculture and intercropped artificial grasslands. *Front. Plant Sci.* 13, 958852. <https://doi.org/10.3389/fpls.2022.958852>.
- Wang, Y., Jia, Y., Guan, L., Lu, C., Lei, G., Wen, L., Liu, G., 2013. Optimising hydrological conditions to sustain wintering waterbird populations in Poyang Lake National Natural Reserve: implications for dam operations. *Freshw. Biol.* 58 (11), 2366–2379.
- Wang, G., Huang, W., Zhou, G., Mayes, M.A., Zhou, J., 2020. Modeling the processes of soil moisture in regulating microbial and carbon-nitrogen cycling. *J. Hydrol.* 585, 124777. <https://doi.org/10.1016/j.jhydrol.2020.124777>.
- Warszawski, L., Frieler, K., Huber, V., Piontek, F., Serdeczny, O., Schewe, J., 2014. The inter-sectoral impact model intercomparison project (ISI-MIP): project framework. *Proc. Natl. Acad. Sci.* 111 (9), 3228–3232. <https://doi.org/10.1073/pnas.1312330110>.
- Wassen, M.J., de Boer, H.J., Fleischer, K., Rebel, K.T., Dekker, S.C., 2013. Vegetation-mediated feedback in water, carbon, nitrogen and phosphorus cycles. *Landsc. Ecol.* 28, 599–614. <https://doi.org/10.1007/s10980-012-9843-z>.
- Willmott, C.J., Robeson, S.M., Matsuura, K., 2012. A refined index of model performance. *Int. J. Climatol.* 32 (13), 2088–2094. <https://doi.org/10.1002/joc.2419>.
- Yang, Y., Tilman, D., Furey, G., Lehman, C., 2019. Soil carbon sequestration accelerated by restoration of grassland biodiversity. *Nat. Commun.* 10 (1), 718. <https://doi.org/10.1038/s41467-019-08636-w>.
- Yinglan, A., Wang, G., Liu, T., Shrestha, S., Xue, B., Tan, Z., 2019. Vertical variations of soil water and its controlling factors based on the structural equation model in a semi-arid grassland. *Sci. Total Environ.* 691, 1016–1026. <https://doi.org/10.1016/j.scitotenv.2019.07.181>.
- Yu, L., Ahrens, B., Wutzler, T., Schrumppf, M., Zaehle, S., 2020. Jena soil model (JSM v1.0; revision 1934): a microbial soil organic carbon model integrated with nitrogen and phosphorus processes. *Geosci. Model Dev.* 13 (2), 783–803. <https://doi.org/10.5194/gmd-13-783-2020>.
- Zedler, J.B., Kercher, S., 2005. Wetland resources: status, trends, ecosystem services, and restorability. *Annu. Rev. Environ. Resour.* 30, 39–74. <https://doi.org/10.1146/annurev.energy.30.050504.144248>.
- Zhang, Y., Lavallee, J.M., Robertson, A.D., Even, R., Ogle, S.M., Paustian, K., Cotrufo, M.F., 2021. Simulating measurable ecosystem carbon and nitrogen dynamics with the mechanistically defined MEMS 2.0 model. *Biogeosciences* 18 (10), 3147–3171. <https://doi.org/10.5194/bg-18-3147-2021>.